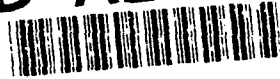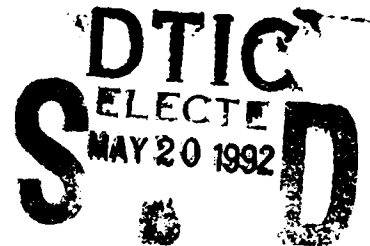AD-A251 240

PL-TR-92-2042

TGAL-91-09

PATH-CORRECTED BODY-WAVE MAGNITUDES AND YIELD ESTIMATES OF NOVAYA ZEMLYA EXPLOSIONS

Rong-Song Jih
Robert A. Wagner
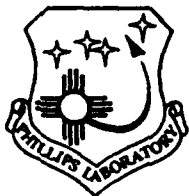
Teledyne Geotech Alexandria Laboratory
314 Montgomery Street
Alexandria, VA 22314-1581

31 AUGUST 1991

DTIC
ELECTE
MAY 20 1992
S D

SCIENTIFIC REPORT NO. 1

92-13346

92 5 19 016

The views and conclusions contained in this document are those of the authors and should not be interpreted as representing the official policies, either expressed or implied, of the Air Force or the U.S. Government.

This technical report has been reviewed and is approved for publication.

JAMES F. LEWKOWICZ
Contract Manager
Solid Earth Geophysics Branch
Earth Sciences Division

JAMES F. LEWKOWICZ
Branch Chief
Solid Earth Geophysics Branch
Earth Sciencs Division

DONALD H. ECKHARDT, Director
Earth Sciences Division

REPORT DOCUMENTATION PAGE

Form Approved
OMB No. 0704-0188

1. AGENCY USE ONLY (Leave blank)	2. REPORT DATE	3. REPORT TYPE AND DATES COVERED
	31 August 1991	Scientific Report, 1 Aug 1990 - 31 Jul 1991

4. TITLE AND SUBTITLE

Path-corrected Body-wave Magnitudes and Yield Estimates of Novaya Zemlya Explosions

5. FUNDING NUMBERS

Contract F19628-90-C-0158

PE 62101F
PR 7600
TA 09
WU AT

6. AUTHOR(S)

R.-S. Jih and R. A. Wagner

7. PERFORMING ORGANIZATION NAME(S) AND ADDRESS(ES)

Teledyne Geotech Alexandria Laboratory
314 Montgomery Street
Alexandria, VA 22314-1581

8. PERFORMING ORGANIZATION REPORT NUMBER

TGAL-91-09

9. SPONSORING/MONITORING AGENCY NAME(S) AND ADDRESS(ES)

Phillips Laboratory
Hanscom AFB, MA 01731-5000
Contract Manager: J. Lewkowicz/GPEH

10. SPONSORING/MONITORING AGENCY REPORT NUMBER

PL-TR-92-2042

11. SUPPLEMENTARY NOTES

12a. DISTRIBUTION/AVAILABILITY STATEMENT

Approved for Public Release; Distribution Unlimited

12b. DISTRIBUTION CODE

13. ABSTRACT (Maximum 200 words)

Along with an extensive data set of worldwide explosions recorded at WWSSN, teleseismic short-period body-wave amplitudes from 28 Novaya Zemlya explosions are measured and analyzed to isolate the propagation characteristics and to derive a better measure of the source size. The separation of path effects from station effects provides direct clues as how an old fold-belt structure (like Novaya Zemlya) could "modulate" the short-period P-wave amplitude and travel-time patterns. A strong correlation between P-wave amplitude and L_g detection at teleseismic distance is also observed. Assuming the basic coupling and the mantle condition at Novaya Zemlya are comparable to those at Eastern Kazakhstan, the m_b bias relative to NTS at 50KT level using the path-corrected $m_b(P_{max})$ values is inferred as 0.25 and 0.36 magnitude unit for Novaya Zemlya and Semipalatinsk, respectively. The $m_b(P_{max})$ bias of 0.11 between Semipalatinsk and Novaya Zemlya could be largely due to the difference in pP interference at these two test sites. The relative source size determined by Burger et al. (1986) and the theoretical Ψ_∞ yield scaling are combined to extrapolate our m_b scaling to the higher end. The resulting yield estimates range from 2 to 2100 KT, with peak values at 550 KT and 65 KT before and after 1976, respectively, which are in reasonable agreement with those in previous studies.

14. SUBJECT TERMS

Body-wave Magnitude, Yield Estimation, Station Amplification, Path Effect, m_b Bias, $m_b(L_g)$, General Linear Model, Maximum-likelihood Inversion

15. NUMBER OF PAGES

72

16. PRICE CODE

17. SECURITY CLASSIFICATION OF REPORT	18. SECURITY CLASSIFICATION OF THIS PAGE	19. SECURITY CLASSIFICATION OF ABSTRACT	20. LIMITATION OF ABSTRACT
Unclassified	Unclassified	Unclassified	UL

(THIS PAGE INTENTIONALLY LEFT BLANK)

Table of Contents

List of Figures

List of Figures

List of Tables

SUMMARY

The standard procedure used in estimating the source size of underground nuclear explosions using m_b measurements has been to separate the station terms from the network-averaged source terms. The station terms thus derived actually reflect the combination of the path effect and the station effect, when only those events in a close proximity are utilized. If worldwide explosions are used in the inversion, then the path effect tends to be averaged out at each station. In either case, the effect due to the propagation path alone would not be obvious.

Under this research contract (**F19628-90-C-0158**) with emphasis on the study of seismic wave propagation in Eurasia, we further decompose the station amplification effect with a joint inversion scheme which simultaneously determines the seismic source size, the path terms, and the receiver terms. Short-period P-wave amplitudes of 217 worldwide underground nuclear explosions, including 28 blasts from Novaya Zemlya, recorded at 118 WWSSN stations have been used in one single inversion to isolate the propagation complexities affecting the P-wave amplitudes. For all 28 Novaya Zemlya events in our WWSSN database, the new m_b factoring procedure provides more stable m_b measurements across the whole recording network with a reduction in the fluctuational variation by a factor of up to 3. Typical reduction factor in the variation is about 2. The the worst case of 1.26 turns out to be a double explosion.

The inferred path terms are then compared against the travel-time residuals to characterize the propagation paths. Our result indicates that paths from the northern test site in Novaya Zemlya to stations in North America have systematically faster arrivals and smaller amplitudes, suggesting a profound defocusing effect on the first arrivals; while stations in Ireland, Scotland, Spain, Bangladesh, northern India, Pakistan, Korea, and Kenya report slow arrivals and large amplitudes, suggesting a focusing effect. Amplitudes for paths to Greenland, Iceland, Alaska, Turkey, Germany, Luzon, Zimbabwe, Italy, Puerto Rico, Ethiopia, and Hawaii, however, seem to be controlled by the anelastic attenuation with slow rays also associated with small amplitudes, and fast rays associated with large amplitudes. The separation of path effects from station effects provides direct clues as how an old fold-belt structure (like Novaya Zemlya) could "modulate" the short-period P-wave amplitude and travel-time patterns. A strong correlation between the P-wave amplitude and L_g detection at teleseismic distance is also observed.

As a byproduct of this study, we have derived the yield estimates of Novaya Zemlya explosions based on the path-corrected m_b values. Assuming the basic coupling and the mantle condition at Novaya Zemlya are comparable to those at Eastern Kazakhstan, the m_b bias relative to NTS at 50KT level using the path-corrected $m_b(P_{max})$ values is inferred as 0.25 and 0.36 magnitude unit for Novaya Zemlya and Semipalatinsk, respectively. The $m_b(P_{max})$ bias of 0.11 between Semipalatinsk and Novaya Zemlya could be largely due to the difference in pP interference between these two test sites (rather than the seismic coupling). The relative source size determined by Burger *et al.* (1986) and the theoretical Ψ_∞ :yield scaling are combined to extrapolate our m_b scaling to the higher end. The resulting yield estimates of Novaya Zemlya explosions range from 2 to 2100 KT, with peak values at 550 KT and 65 KT for events before and after 1976, respectively, which are in reasonable agreement with those in previous studies.

Also included in this report is a complete listing of path-corrected m_b values and yield estimates of Semipalatinsk explosions which are used as our baseline in calibrating Novaya Zemlya explosions. First motion of the initial short-period P waves appears to be a very favorable source measure for explosions fired in hard rock sites underlain by the stable mantle (such as Semipalatinsk).

1. INTRODUCTION

The seismic data from the northern nuclear test site in Novaya Zemlya (hereby denoted by NNZ) are important in part because nuclear tests at the (relatively more understood) Semipalatinsk test site in Eastern Kazakhstan (hereby denoted by KTS) probably will not be resumed, and that several large historical explosions were detonated at Novaya Zemlya. Many seismological problems associated with Novaya Zemlya tests still need to be studied with various approaches.

There are fundamental differences in the energy flux in short-period P waves from underground explosions at different test sites. These differences reflect both near-source conditions (such as the effect of local rock competence on pP delay time), regional conditions (such as the shallow high-velocity defor using body beneath Pahute Mesa), and global conditions (such as the deep mantle heterogeneity producing the common pattern in the Nevada Test Site [NTS] P waves and P coda (Lay and Welc, 1987). Novaya Zemlya is a very interesting test site in terms of the seismic propagation characteristics. For instance, all Novaya Zemlya explosions recorded at YKA have complex waveforms (Douglas et al., 1973), and similar (complex) signals from the same test site have been recorded at other stations in North America (Butler and Ruff, 1980). We here present our Novaya Zemlya results based on the body-wave magnitude study to explain some of the complexity in propagation observed previously.

The body wave magnitudes used in developing and applying the magnitude-yield relationship are network m_b values which are some "average" of the station m_b. Previously a major objective of magnitude-calculation research was to determine the network m_b that is not biased by the sample truncation due to the limited range of the seismometers. Ringdal (1976) introduced the maximum-likelihood estimator [MLE] to correct for the statistical bias introduced by data censoring from non-detection. Von Seggern and Rivers (1978) pointed out the importance of accounting for the data censoring due to signal clipping. Blandford and Shumway (1982) derived the general linear model [GLM] in the presence of data censoring using the Expectation Maximization [EM] algorithm. They simultaneously estimated event magnitudes and station corrections in a maximum-likelihood sense. Jih and Shumway (1989) re-examined and documented the GLM algorithms, and they discussed the uncertainty assessment in the censoring situation. It is concluded that in the multi-parameter linear regression problem with censored data, the scaling of $\sigma/\sqrt{\text{degrees of freedom}}$ still provides an extremely good approximation of the uncertainty associated with each parameter. In the case of non-

censoring, such approximation can be proved to be "exact". The methodological similarities and differences between the iterative least squares [ILS] and the maximum-likelihood estimator [MLE] were also identified in Jih and Shumway (1989).

Jih and Wagner (1991b) propose to compute the new station magnitude $m_{2.9}$ for the i-th event recorded at the j-th station as

$$m_{2.9}(i,j) = \log_{10}[A(i,j)/T(i,j)] + B(\Delta(i,j)) - S(j) - F(k(i),j)$$

where $A(i,j)$ is the displacement amplitude (in millimicrons) and $T(i,j)$ is the period (in seconds) of the P wave. The $B(\Delta)$ is the distance-correction term. $S(j)$ is the station correction, and $F(k(i),j)$ is the path correction for explosions from the $k(i)$-th source region. The resulting new magnitude is called $m_{2.9}$ to avoid confusion with the m_3 defined in Marshall et al. (1979) that corrects for the source-region attenuation and station terms solely based on published P_n velocity. The path corrections determined in this procedure provide direct and informative clues to characterize the various propagation paths. We will also use $m_{2.9}$ extensively throughout this study to characterize the scaling relationship with other magnitude measurements and to make the yield estimates.

2. PATH-CORRECTED UNBIASED NETWORK m_b ESTIMATOR

The conventional definition of station magnitude is computed as

$$m_b = \log_{10}(A/T) + B(\Delta) \qquad [1]$$

where A is the displacement amplitude (in nm) and T is the predominant period (in sec) of the P wave. The $B(\Delta)$ is the distance-correction term that compensates for the change of P-wave amplitudes with distance (e.g., Gutenberg and Richter, 1956; Veith and Clawson, 1972). m_b in [1] is also denoted as m_1 in Marshall et al. (1979). The ISC bulletin m_b is just the network average of these raw station m_b values without any further adjustment.

Consider N_E explosions detonated at N_F source regions that are recorded at some or all of N_S stations. The conventional GLM [General Linear Model] or LSMF [Least Squares Matrix Factorization] network m_b (Douglas, 1966; Ericsson, 1971; von Seggern, 1973; Blandford and Shumway, 1982; Marshall et al.,1984; Jih and Shumway, 1989; Murphy et al., 1989) is the least-squares or maximum-likelihood network average of the "station-corrected" magnitudes:

$$m_{2.2}(i,j) \equiv m_1(i,j) - S(j) \qquad [2]$$

where S(j) is the "statistical" or "empirical" receiver correction at the j-th station. In Marshall et al. (1979), a priori information about the P_n velocity underneath each station is used to determine its associated "deterministic" receiver correction, S(j), and the resulting magnitude is called m_2. The GLM receiver corrections, however, are inferred jointly from a suite of event-station pairs, and no a priori geophysical or geological condition is assumed (and hence the different notation $m_{2.2}$). The high correlation between the tectonic type and the GLM station terms suggests that the empirical station corrections do reflect the averaged upper mantle conditions underneath the receivers, if the azimuthal coverage at each station is broad enough.

Jih and Wagner (1991b) propose to compute the new station magnitude $m_{2.9}$ for the i-th event recorded at the j-th station as

$$m_{2.9}(i,j) \equiv m_1(i,j) - S(j) - F(k(i),j) = m_{2.2}(i,j) - F(k(i),j) \qquad [3]$$

At the j-th station, F(k(*),j) is a constant for all events detonated in the same k-th "geologically and geophysically uniform region". Partitioning a single nuclear test site into several "regions" may be necessary in order to account accurately for the focusing/defocusing effects. This $m_{2.9}$ is very similar to the m_3 in Marshall et al. (1979) except that, again, a priori attenuation information of the source region is used in Marshall et al. (1979) to determine the

correction term, whereas Jih and Wagner (1991b) invert for the path or near-source effects from the data empirically. In other words, the source-region corrections proposed by Marshall *et al.* (1979) are constants (for all explosions in the same source region) regardless of the location of the seismic stations, whereas the path/near-source corrections in Equation [3] are highly dependent on the source-station paths.

We now examine briefly the fundamental difference between the present scheme (Equation [3]) and the previous GLM schemes. In LSMF and the standard GLM schemes (*e.g.*, Douglas, 1966; Ericsson, 1971; von Seggern, 1973; Blandford and Shumway, 1982; Marshall *et al.*, 1984; Lilwall *et al.*, 1988; Jih and Shumway, 1989; Murphy *et al.*, 1989), it is assumed that the observed station $m_b(i,j)$ is the sum of the true source size of the i-th event, $E(i)$, the receiver term of the j-th station, $S(j)$, and the random noise, $v(i,j)$:

$$m_b(i,j) = E(i) + S(j) + v(i,j) \qquad [4]$$

The receiver term, $S(j)$, is constant with respect to all explosions from different test sites, and hence it would inherently reflect the "averaged" receiver effect --- provided the paths reaching the station have broad azimuthal coverage. When world-wide explosions are used, the standard deviation (σ) of the noise v in [4] is typically about 0.3 m.u. or larger.

If LSMF or GLM is applied to events within a smaller area of source region, then the σ of v in [4] could reduce to 0.15-0.2 m.u. However, the result of such "single-test-site GLM" approach should be interpreted or utilized cautiously. The m_b values so determined are excellent estimates of "relative source size" for that test site only. If this "single-test-site GLM" inversion is applied to several test sites separately, it may not be easy or obvious to find a consistent baseline for "absolute yield" estimation or immediate combination of the (inter-site) magnitudes, since the recording network is typically different from one test site to another, and hence the station terms are inevitably inconsistent. Furthermore, the station terms derived by the "single-test-site GLM" may not necessarily represent the attenuation underneath the receiver side alone. They could be contaminated or sometimes even overwhelmed by the path/near-source effects shared by the explosions confined in a narrow azimuthal range. This could explain the once puzzling and controversial phenomenon Butler and Ruff (1980) (also Butler, 1981; Burdick, 1981) reported, namely that using Soviet explosions from one test site alone may fail to discern the attenuation differential between the eastern and western U.S. There is no doubt, however, that the GLM or LSMF type of methodology can infer the station terms which are strongly correlated with the upper mantle attenuation underneath the stations, provided the seismic sources have a broad spatial coverage as did those in North (1977), Douglas and Marshall (1983), Lilwall and Neary (1985), Ringdal (1986), Jih

- 4 -

and Wagner (1991b), and many others.

In the present scheme ([3]), however, we reformulate the whole model as

$$m_b(i,j) = E(i) + S(j) + F(k(i),j) + v(i,j) \qquad [5]$$

where $F(k(i),j)$ is the correction term at the j-th station for the propagation effect or the near-source focusing/defocusing effect, which is constant for all events in the k-th "geologically and geophysically uniform region". For each seismic station, this F can be regarded as its azimuthal variation around the mean station term S. However, as explained previously, it would be more appropriate to consider F the path or near-source term because the back azimuths at the station could be nearly identical for adjacent test sites (such as Degelen and Murzhik), and yet the "F" terms could be very different. By incorporating the F term into the model, the σ for world-wide explosions is reduced to about 0.2, roughly the same level that which a "single-test-site GLM" could achieve. Intuitively, the present scheme (Equations [3] or [5]) provides a more detailed (and hence better) model than that of Equation [4] in describing the whole propagation path from the source towards the receiver. Simply put, Equation [4] yields a stronger fluctuation in the source terms, E, as well as a larger standard deviation of v because each term in the right-hand side of Equation [4] would have to "absorb" part of the missing F term in [5]. This is exactly the same reason why $m_{2.2}$ has smaller variation than m_1.

Roughly speaking, the procedure described in [3] has the following advantages:

- It provides more stable m_b measurements across the whole recording network, as compared to the conventional GLM or LSMF procedure which only corrects for the station terms. The reduction in the standard deviation of network m_b from m_1 to $m_{2.9}$ could reach a factor of nearly 3 (Figures 1 and 2). As a result, the scatter in $m_{2.9}$ versus log(yield) is smaller than that for other m_b, as illustrated by Jih and Wagner (1991b) with Semipalatinsk explosions.

- The resulting network m_b values are not significantly different from the GLM results (cf. Figures 4 through 8). Thus if the network m_b values derived by GLM or LSMF are unbiased, so are the refined results.

- The separation of the path effect from the station effect is a crucial step to study the various propagation phenomena, which in turn would improve our understanding of the seismic source as well.

We have applied this procedure to 217 worldwide explosions, including 28 blasts from northern subsite of Novaya Zemlya, and the resulting $m_{2.9}$ values are listed in Table 1. The

118 WWSSN [World Wide Standarized Seismograph Network] stations are selected such that each station records 10 or more good explosion signals. There are 13840 signals, 9080 noise measurements, and 1609 clips from 17 test sites that are used to invert for the 2733 unknown parameters with the maximum-likelihood approach. The standard deviation of $v(i,j)$ in [5] is 0.196, as compared to 0.294 if the conventional GLM (Equation [4]) is applied to the same data set. A complete list of the event magnitudes and the path corrections for each test site can be found in Jih and Wagner (1992). Here we limit the discussion to Novaya Zemlya explosions only.

Table 1. Path-corrected m_b of Novaya Zemlya Explosions						
Event		# of Signals[1]	Magnitudes			
Date	Site	Ns Nn Nc	S.E.M.[2]	$m_b(P_a)$	$m_b(P_b)$	$m_b(P_{max})$
661027	NNZ	56 0 13	0.024	6.069	6.305	6.451
671021	NNZ	53 5 3	0.025	5.422	5.610	5.781
681107	NNZ	58 1 5	0.024	5.603	5.847	6.031
691014	NNZ	59 2 7	0.024	5.768	5.962	6.132
701014	NNZ	35 0 22	0.026	6.438	6.631	6.808
710927	NNZ	23 0 21	0.029	6.243	6.442	6.579
720828	NNZ	32 0 11	0.030	5.983	6.232	6.367
730912	NNZ	23 0 21	0.029	6.363	6.679	6.772
740829	NNZ	25 0 18	0.030	6.140	6.386	6.569
751021	NNZ	23 0 17	0.031	6.104	6.330	6.532
750823	NNZ	27 0 12	0.031	6.151	6.389	6.507
760929	NNZ	27 4 7	0.032	5.250	5.466	5.600
761020	NNZ	25 34 0	0.025	4.258	4.509	4.784
770901	NNZ	25 2 2	0.036	5.165	5.461	5.596
771009	NNZ	18 22 0	0.031	4.225	4.320	4.537
780810	NNZ	39 3 18	0.025	5.412	5.639	5.865
780927	NNZ	42 7 10	0.025	5.105	5.362	5.524
790924	NNZ	39 2 16	0.026	5.292	5.553	5.739
791018	NNZ	39 7 14	0.025	5.305	5.500	5.698
801011[3]	NNZ	42 4 6	0.027	5.188	5.439	5.667
811001	NNZ	43 4 5	0.027	5.278	5.512	5.674
821011	NNZ	32 11 5	0.028	5.123	5.292	5.444
830818	NNZ	30 4 5	0.031	5.316	5.521	5.706
830925	NNZ	31 4 5	0.031	5.248	5.467	5.644
841025	NNZ	22 3 4	0.036	5.191	5.461	5.624
870802	NNZ	22 3 6	0.035	5.318	5.529	5.687
880507	NNZ	20 4 1	0.039	5.133	5.311	5.460
881204	NNZ	15 4 2	0.043	5.279	5.548	5.677

1: Ns = # of signals, Nn = # of noise measurements, Nc = # of clips.

2: standard error in the mean.

3: double explosion.

The average offset between our $m_b(P_b)$ values of the 11 events before 1976 and those in Burger *et al.* (1986) (also measured from the P_b phase) is -0.042 ± 0.017 magnitude unit [m.u.]. Using the *RMS* L_g measured at NORSAR (Ringdal and Fyen, 1991; Ringdal and Marshall, 1989) as a reference, there appears to be a $m_b(P_{max})-L_g$ bias of 0.1 m.u. between Novaya Zemlya and Eastern Kazakh. This bias becomes negligible, however, if $m_b(P_a)$ is used to compare with $m_b(L_g)$ (instead of using the conventional peak-to-peak amplitudes) (*cf.* Table 2). Comparison with Nuttli's (1986b, 1988) $m_b(L_g)$ gives very similar result (Table 3). The indifference of $m_b(P_a)-L_g$ between KTS and NNZ indicates that perhaps these two test sites have very comparable basic seismic coupling; and that the discrepancy in $m_b(P_{max})$ excitation (relative to L_g) could be due to different pP interference. We will give the yield estimates of Novaya Zemlya explosions based on this hypothesis in a later section.

As a side remark, there is a significant difference in $m_b(P_{max})-RMS\ L_g$(NORSAR) between southwestern (SW) and northeastern (NE) subsites of Balapan, as discussed in many other studies. The value of 0.11 m.u. shown here is slightly smaller than that of previous studies, though. Regressions with yields published by Bocharov *et al.* (1989) show that NE explosions have positive L_g residuals and negative m_b residuals; whereas SW explosions show the opposite trend (Jih and Wagner, 1991b, 1992). Thus it would seem plausible that the apparent m_b-L_g bias could be "enhanced" by the negative correlation between m_b and L_g residuals. It is interesting to note the much smaller m_b-L_g bias when P_a is used (Table 2). A three-dimensional geological model of the Balapan test site by Leith and Unger (1989) shows a distinct difference between the NE and SW portions of the test site, with the granites closer to the surface and the alluvium thinner in the southwest (see also Bonham *et al.*, 1980). The thicker alluvium layer in NE region could increase the waveform complexity (as first observed by Marshall *et al.*, 1984) and reduce the magnitudes measured with P_{max}. Nevertheless, the first motion (*i.e.*, P_a) should be least affected by this factor, and therefore a favorable source measure --- so long as it is not contaminated by the microseismic noise at the receiver site.

Nuttli (1987, 1988) suggests that there is a m_b bias of about 0.2 m.u. between Degelen and Balapan, with Degelen explosions having even larger m_b excitation (relative to L_g). We do not see such Degelen-Balapan bias with *RMS* L_g measured at NORSAR (Table 2). The Degelen data set alone is too small for decisive conclusion. However, if we treat Murzhik as part of Degelen, as did Nuttli (1987), the average $m_b(P_{max})-RMS\ L_g$(NORSAR) bias between Degelen and Balapan is only 0.02 m.u., which is insignificant.

Table 2. $m_{2.9}$-RMS L_g(NORSAR) at Various Sites			
Site*	$m_b(P_a)-m_b(L_g)$, #	$m_b(P_b)-m_b(L_g)$, #	$m_b(P_{max})-m_b(L_g)$, #
BSW	-0.504±0.011 11	-0.228±0.011 11	+0.023±0.015 20
BNE	-0.565±0.023 8	-0.304±0.014 9	-0.092±0.012 14
BTZ	-0.523±0.045 6	-0.243±0.020 6	-0.041±0.015 14
Deg	-0.484±0.046 5	-0.207±0.042 5	+0.012±0.034 5
Mzk	-0.562±0.073 3	-0.259±0.045 3	-0.046±0.032 3
KTS	-0.524±0.013 33	-0.250±0.010 34	-0.026±0.010 56
NNZ	-0.519±0.020 14	-0.296±0.023 14	-0.121±0.024 14

*: BSW = SW subsite, Balapan; BNE = NE subsite, Balapan; BTZ = transition zone, Balapan; Deg = Degelen Mountain; Mzk = Murzhik; KTS = all 5 subsites in Eastern Kazakh combined; NNZ = northern subsite, Novaya Zemlya.

Table 3. $m_{2.9}$-$m_b(L_g)$ (Nuttli) at Various Sites			
Site	$m_b(P_a)-m_b(L_g)$, #	$m_b(P_b)-m_b(L_g)$, #	$m_b(P_{max})-m_b(L_g)$, #
BSW	-0.544±0.050 8	-0.244±0.040 8	-0.034±0.028 16
BNE	-0.584±0.043 6	-0.303±0.039 7	-0.075±0.031 14
BTZ	-0.444±0.078 5	-0.184±0.057 5	-0.033±0.024 13
Deg	-0.524±0.124 5	-0.196±0.112 5	+0.050±0.100 5
KTS	-0.529±0.033 24	-0.239±0.028 25	-0.037±0.017 48
NNZ	-0.549±0.033 24	-0.324±0.035 24	-0.151±0.032 24

3. RECEIVER AND PATH EFFECTS ON P WAVES FROM NOVAYA ZEMLYA

Figure 1 shows our receiver terms which are inferred jointly along with the source-size estimates and path terms from the worldwide explosions. The receiver corrections derived with this approach match the average tectonic structure underneath each station very well, mainly due to the broad coverage of azimuths at each station. Generally speaking, the station terms are positive in shield regions such as Australia, Canada, India, and Scandinavia, and they are negative in the east Africa rift valleys, mid-ocean ridges (e.g., Iceland and Azores Islands), island arcs (e.g., Indonesia, Japan, and Taiwan), and Himalaya Mountain Ranges (Chaman Fault, northern India, Nepal, and Burman Arc). Solomon and Toksoz (1970) and many other studies (e.g., Evernden and Clark, 1970; Booth et al., 1974) found that for stations in U.S., the attenuation is higher between the Rockies and Cascades, and in the northeastern U.S. This pattern is also observable in Figure 1 (see also North, 1977). Jih and Wagner (1992) compare these empirically determined station terms with those predicted by Marshall et al. (1979) based on published P_n velocity, and find that they match rather well. As North (1977) put it, it is gratifying that a simple parameter such as m_b can be utilized to reveal the tectonics. It should be noted, however, that our empirical station terms also include the effect due to the crustal amplification if such local site effect is shared by all ray paths from different test sites to a particular station. This could be the reason of a few outliers such as HNR (Honiara, Solomon Islands), PMG (Port Moresby, East Papua New Guinea), RAB (Rabaul, New Britain), and BAG (Baguio City, Luzon, Philippines) which do not show negative station terms as would be expected from the strong seismicity in that region (cf. Figure 1). Another possible reason is that these stations have relatively poorer azimuthal sampling in our data set, and hence the station bias at these three stations is not well constrained.

Figure 2 shows the map of the "pure propagation effect" (top) and the combined station amplification (bottom) defined as the sum of the receiver term in Figure 1 and the path effect for Novaya Zemlya explosions. The path term at each station can be regarded as the azimuthal variation (towards the various source regions) relative to the averaged station amplification.

We also applied the joint inversion scheme to the travel-time residual data set. Although there are much fewer events in our database for which the accurate WWSSN travel-time residuals are available, the multiple events from each test site still permits the reliable separation of path and station effects. The detailed discussion of the global result is deferred to Jih and Wagner (1992), and only the result of Novaya Zemlya is presented here. Figure 3 is a map

- 10 -

showing the product of the travel-time residual and the magnitude residual at each station. Only the path term of each ray is used. Thus positive symbols represent the paths that encounter some focusing or defocusing structure, whereas the negative symbols are those paths dominated by attenuation mechanism. The paths from Novaya Zemlya to stations in North America have systematically faster arrivals and smaller amplitudes, suggesting a profound defocusing effect on the first arrivals; while stations in Ireland, Scotland, Spain, Bangladesh, northern India, Pakistan, Korea, and Kenya report slow arrivals and large amplitudes, suggesting a focusing effect. Amplitudes for paths to Greenland, Iceland, Alaska, Turkey, Germany, Luzon, Zimbabwe, Italy, Pueto Rico, Ethiopia, and Hawaii, however, seem to be controlled by the anelastic attenuation with slow rays also associated with small amplitudes, and fast rays associated with large amplitudes. The crust beneath the Arctic Ocean floor is composed of oceanic basins (including the Canada Basin, Makarov Basin, Fram Basin, and Nansen Basin) which are all are located in nearly parallel positions and are separated by the Alpha Ridge, Lomonosov Ridge, and Arctic Mid-Ocean Ridge (Nansen-Gakkel Ridge) (Perry *et al.*, 1986). Focusing and defocusing effects of surface waves propagating across the region have been observed in earlier seismic studies (*e.g.*, Zeng *et al.*, 1986). Perhaps the upper mantle underneath these oceanic ridges has some complex features which cause the strong defocusing effect across many WWSSN stations in North America as observed in Figures 2 and 3.

Butler and Ruff (1980) examined SP *P*-wave amplitudes of Novaya Zemlya explosions recorded by WWSSN stations in U.S. The lowest amplitudes were found in GOL (Golden, Colorado) and ALQ (Albuquerque, New Mexico), with a factor of 4 lower than high amplitudes. Our study with enlarged data set recorded at a global network show very consistent result. The stations showing the lowest amplitudes are SHK (Shiraki, southern Honshu, Japan), KTG (Kap Tobin, eastern Greenland), GOL, SJG (San Juan, Puerto Rico region), LEM (Lembang, Java), and ALQ. On the other hand, COP (Copenhagen, Denmark), HLW (Helwan, United Arab Republic), MSH (Mashhad, Iran-Turkmenistan border), IST (Istanbul, Turkey), AQU (Aquila, central Italy), and ESK (Eskdalemuir, United Kingdom) report the highest amplitude for NNZ explosions (Table 4). Note that the station COP, which has the largest combined station amplification for *P* wave from NNZ, is also used in Nuttli's (1986b, 1988) $m_b(L_g)$ study of Balapan and NNZ events. Nuttli (1988) obtained a smaller Q (Q is the elastic quality factor) for paths from NNZ to another Scandinavian station KON (Konsberg, southern Norway) in his $m_b(L_g)$ study. It is interesting to note that KON has negative path term in our analysis (Table 4). The high correlation between the signal strengths of teleseismic *P*-wave recordings and that of teleseismic L_g detection is not coincidental, as similar phenomena have been

observed with Semipalatinsk explosions at other stations as well (Jih and Wagner, 1992).

For explosions fired in fold belts such as NZ (in an extension of the Urals fold belts) and at Amchitka site (in the Aleutian arc), Douglas *et al.* (1973) suggest that stations on great-circle paths that lie along the fold belts could show complex signals and small amplitudes. The evidence Douglas *et al.* (1973) see with SI-BC (Smithers, British Columbia) and PG-BC (Prince George, British Columbia) recordings of the Amchitka explosion LONGSHOT points to a low Q zone along the fold belts. The WWSSN station COL (College Outpost, central Alaska) happens to be located on the great-circle path along both fold belts of NNZ and Aleutian, and it does have anomalously small m_b for Amchitka events (Jih and Wagner, 1992) as well as moderately small m_b for NNZ events (Figure 2), which appears to be due to low Q along the propagation paths (Figures 3 and 4) since the station term itself is nearly zero (Table 4). This would seem to be somewhat similar to the pattern Jih and Wagner (1991a) observe for the Murzhik explosions at azimuths towards northwest and southeast, although a defocusing mechanism along the Chingiz Fault near Murzhik test site would be plausible in that case.

Figures 2, 3 and Table 4 show that WWSSN stations in Greenland and Iceland (GDH, Godhavn, western Greenland; KTG, Kap Tobin, eastern Greenland; and AKU, Akureyri, Iceland) have systematically slow arrivals as well as small amplitudes for Novaya Zemlya explosions, which suggests that the low Q mechanism proposed by Douglas *et al.* (1973) is plausible for these paths. Figure 4 shows all earthquakes with $m_b > 4.5$ within 40° from the North Pole. The *P* waves from Matochkin Shar of Novaya Zemlya to these stations have to tunnel through the upper mantle underneath the mid-ocean ridge axis (Greenland Fracture Zone, Mohns Ridge, Jan Mayen Fracture Zone, Jan Mayen Ridge, and Kolbeinsey Ridge), where the anelastic attenuation is expected to be very strong. In fact, the whole Mohns Ridge is right on the path from Novaya Zemlya to AKU, and hence the complexity in the *P*–wave signal is inevitable. Chan *et al.* (1989) also observed extremely low Q_β at WWSSN station AKU with surface-wave recordings. Nevertheless, AKU does report simple waveforms and large amplitudes for explosions fired in Balapan, Degelen, and French Sahara; for these paths are not affected by the mid-ocean ridge (Jih and Wagner, 1992).

Several studies have noted the observed negative correlation between magnitude and complexity: as with earthquake signals, the station magnitude of an explosions measured from a complex signal is smaller than that measured from a simple signal (Davies, 1970). Douglas *et al.* (1973, 1981) propose an explanation of complexity which is similar to that of Davies (1970) except that the direct *P* (and *pP*) is assumed to be strongly attenuated by a region of relatively low Q and that the later arrivals that form the coda of the complex signals are in

- 12 -

effect scattered signals that have traveled by the relatively high Q paths and hence with little attenuation. On this "weak signal" explanation of complexity, the m_b measured from a complex signal should be less than that computed from a simple signal of the same explosion. Our experience in measuring the WWSSN film chips is in general agreement with this theory. Stations with negative combined path and receiver effects do show complex waveforms. LEM is a notorious example for having complex signals and small amplitudes for all Eurasian test sites we studied, including NNZ. Nevertheless, Amchitka explosions recorded at LEM are not complex, despite that LEM is located in a tectonic region.
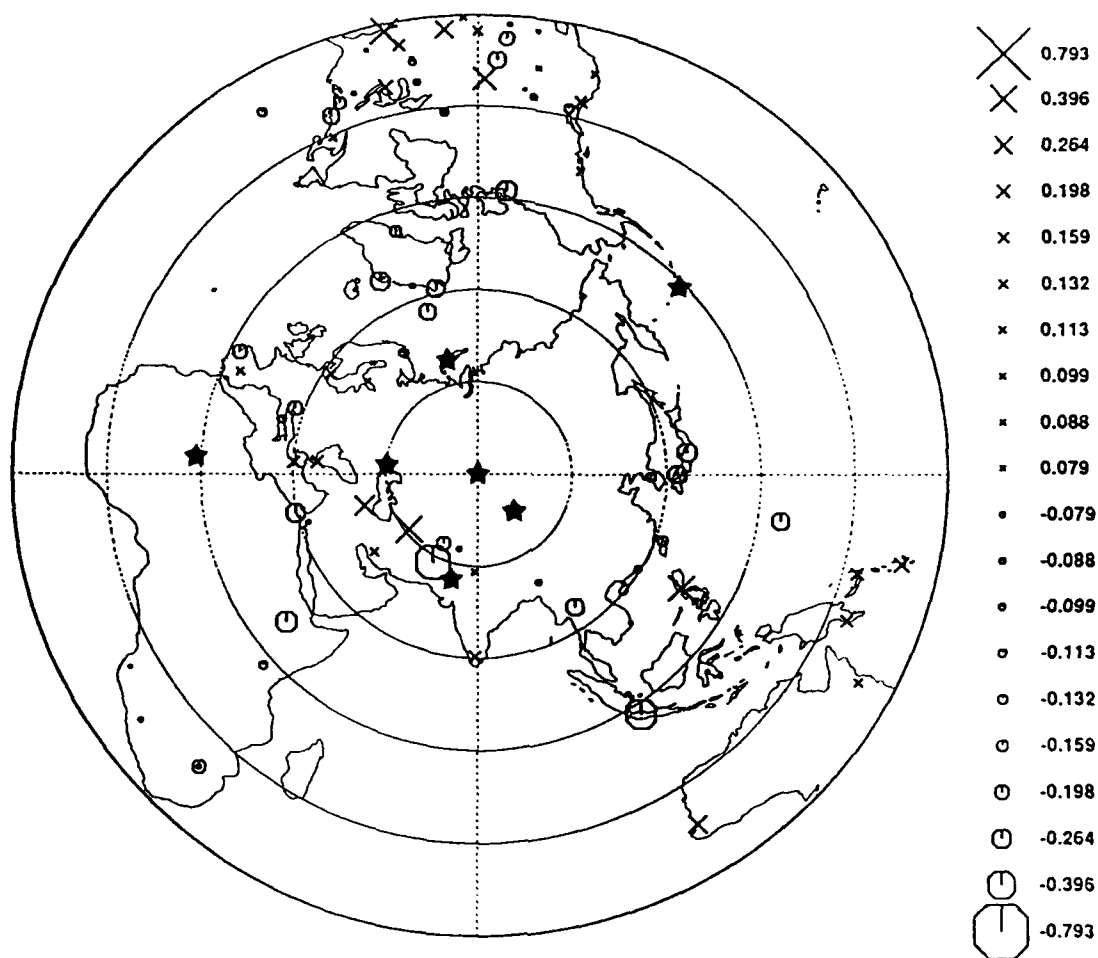
Figure 1. The WWSSN station terms inferred from a GLM/MLE joint inversion scheme which simultaneously inverts for the seismic source sizes, receiver terms, as well as the path effects. The inversion of 2733 unknown parameters is carried out with 13840 signals, 9080 noise measurements, and 1609 clips from 217 worldwide explosions recorded at 118 selected WWSSN stations. Only paths within 20 and 95 *degrees are used.* For each station, our joint inversion scheme regards any component in common across all events as the corresponding "station term", similar to the Douglas' (1966) LSMF approach. The high correlation between the tectonic type and the station terms suggests that these empirical corrections do reflect the upper mantle conditions underneath the receivers. Darkened stars represent some of the nuclear test sites used in this study.
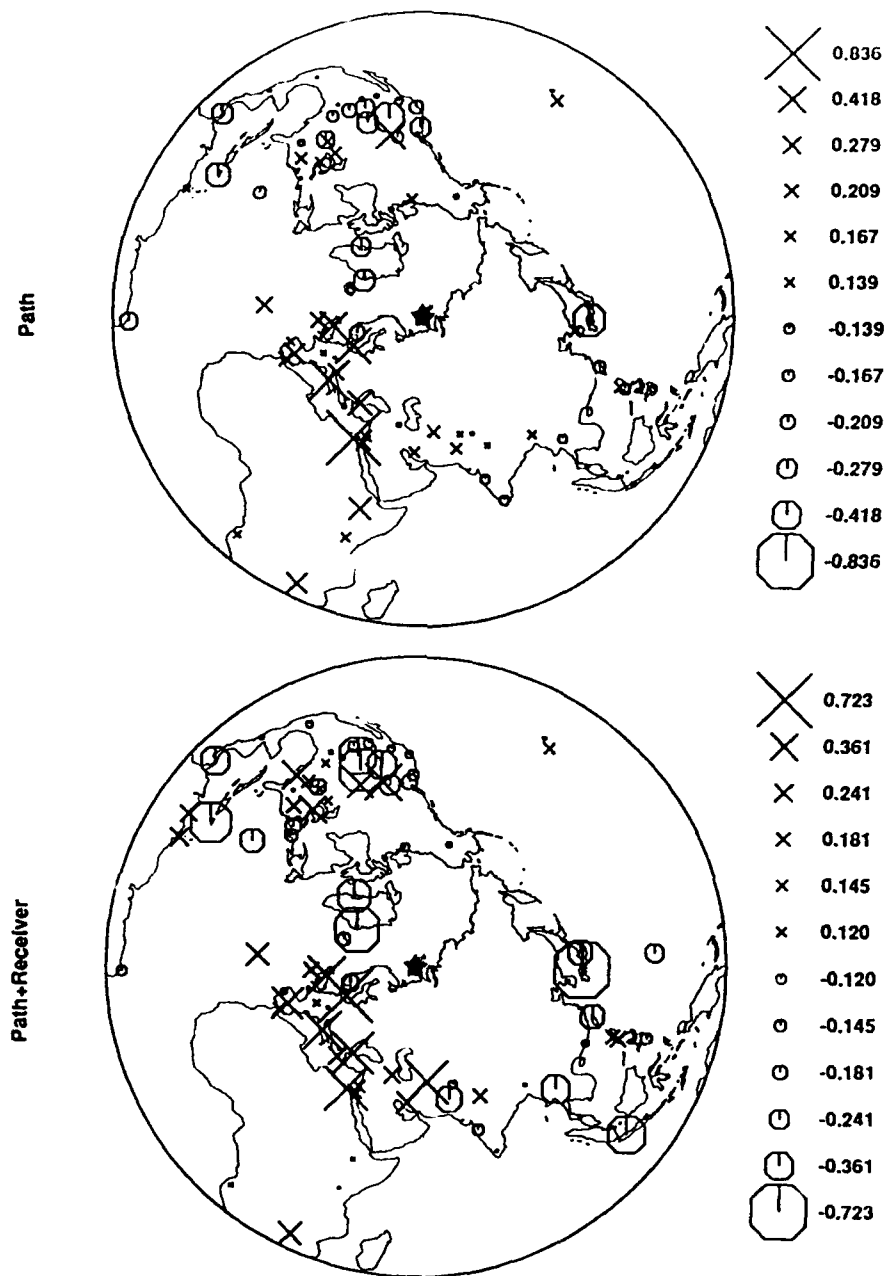
Figure 2. The map showing the "pure propagation effect" (top) and the combined station amplification (bottom) defined as the sum of the receiver term (Figure 1) and the path effect for Novaya Zemlya explosions. The paths from Novaya Zemlya to stations in North America have systematically faster arrivals and smaller amplitudes, suggesting a profound defocusing effect on the first arrivals; while stations in Ireland, Scotland, Spain, Bangladesh, northern India, Pakistan, Korea, and Kenya report slow arrivals and large amplitudes, suggesting a focusing effect. Amplitudes for paths to Greenland, Iceland, Alaska, Turkey, Germany, Luzon, Zimbabwe, Italy, Pueto Rico, Ethiopia, and Hawaii, however, seem to be controlled by the anelastic attenuation with slow rays also associated with small amplitudes, and fast rays associated with large amplitudes.

Figure 3. The map showing the probable dominating mechanism affecting each path from Novaya Zemlya. Positive symbols (crosses) are those paths associated with focusing/defocusing, and the negative symbols are those dominated by the strong/weak anelastic attenuation. Symbol size gives a qualitative measure of the dominating mechanism.
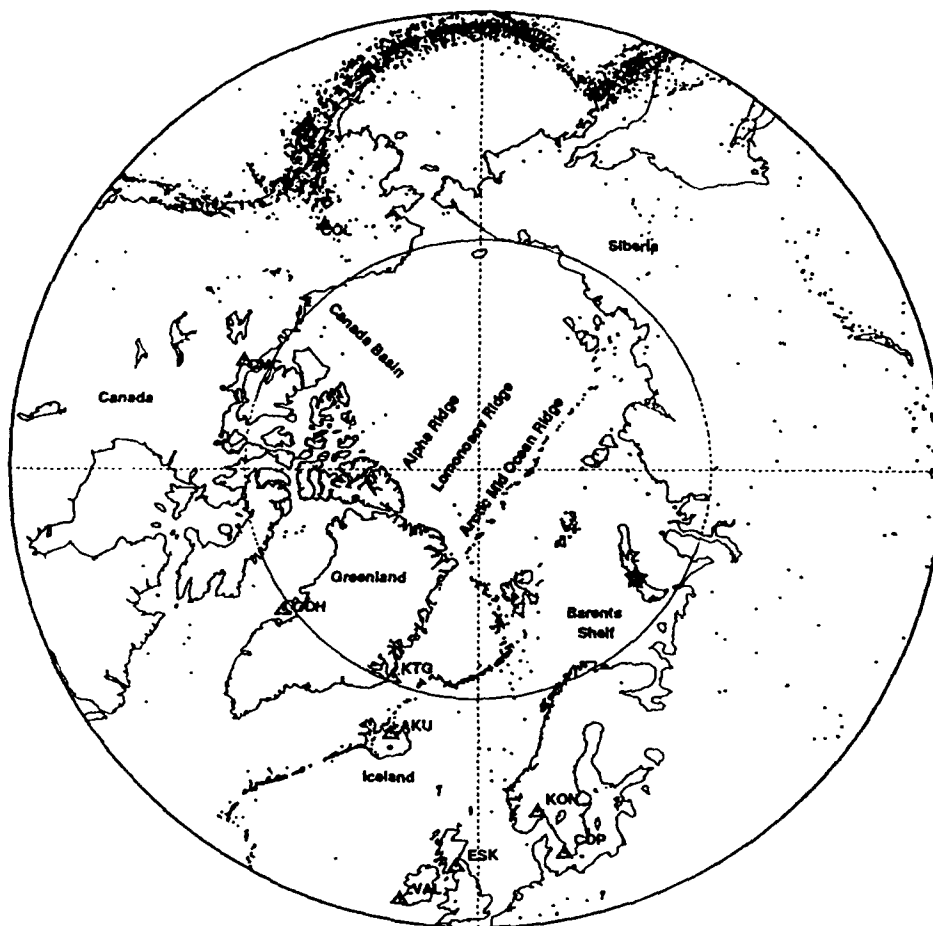
Figure 4. The crust beneath the Arctic Ocean floor is composed of oceanic basins (including the Canada Basin, Makarov Basin, Fram Basin, and Nansen Basin) which are all located in nearly parallel positions and are separated by the Alpha Ridge, Lomonosov Ridge, and Arctic Mid-Ocean Ridge (Nansen-Gakkel Ridge). Remarkable focusing and defocusing effects of surface waves propagating across the region have been observed in earlier seismic studies. The P waves of Novaya Zemlya explosions to stations in Greenland and Iceland have to tunnel through the upper mantle underneath the mid-ocean ridge axis (Greenland Fracture Zone, Mohns Ridge, Jan Mayen Fracture Zone, Jan Mayen Ridge, and Kolbeinsey Ridge), where the anelastic attenuation is expected to be very strong, and hence the complexity in the P-wave signal is inevitable.

Table 4. Receiver and Path Effect on m_b of Novaya Zemlya Events					
Station	Lon	Lat	Rcv	Path	Rcv+Path
SHK	132.678	34.532	-0.250	-0.473	-0.723
KTG	-21.983	70.417	-0.254	-0.321	-0.575
GOL	-105.371	39.700	-0.237	-0.312	-0.549
SJG	-66.150	18.112	-0.173	-0.352	-0.525
LEM	107.617	-6.833	-0.417	-0.066	-0.483
ALQ	-106.457	34.943	-0.199	-0.275	-0.474
GDH	-53.533	69.250	-0.155	-0.275	-0.430
DUG	-112.813	40.195	0.074	-0.446	-0.372
BHP	-79.558	8.961	-0.056	-0.305	-0.361
CHG	98.977	18.790	-0.234	-0.125	-0.359
QUE	66.950	30.188	-0.484	0.161	-0.323
MAT	138.207	36.542	-0.256	-0.056	-0.312
ANP	121.517	25.183	-0.139	-0.164	-0.303
BEC	-64.681	32.379	-0.120	-0.176	-0.296
MSO	-113.941	46.829	-0.091	-0.167	-0.258
GUA	144.912	13.538	-0.232	0.006	-0.226
KON	9.598	59.649	0.000	-0.212	-0.212
OGD	-74.596	41.088	-0.164	-0.039	-0.203
FVM	-90.426	37.984	0.069	-0.266	-0.197
LON	-121.810	46.750	-0.121	-0.074	-0.195
AKU	-18.107	65.687	-0.053	-0.108	-0.161
WES	-71.322	42.385	-0.228	0.067	-0.161
DAV	125.575	7.088	-0.040	-0.101	-0.141
EPT	-106.506	31.772	-0.070	-0.069	-0.139
POO	73.850	18.533	-0.004	-0.135	-0.139
COR	-123.303	44.586	0.161	-0.297	-0.136
NAT	-35.033	-5.117	0.128	-0.250	-0.122
TUC	-110.782	32.310	-0.051	-0.067	-0.118
CMC	-115.083	67.833	-0.270	0.162	-0.108

Table 4. Receiver and Path Effect on m_b of Novaya Zemlya Events					
Station	Lon	Lat	Rcv	Path	Rcv+Path
KBL	69.043	34.541	-0.188	0.087	-0.101
BKS	-122.235	37.877	0.104	-0.202	-0.098
GSC	-116.805	35.302	0.022	-0.113	-0.091
HKC	114.172	22.304	-0.087	-0.001	-0.088
UNM	-99.178	19.329	-0.060	-0.028	-0.088
PTO	-8.602	41.139	-0.193	0.118	-0.075
COL	-147.793	64.900	-0.002	-0.068	-0.070
LUB	-101.867	33.583	0.135	-0.204	-0.069
SCP	-77.865	40.795	-0.060	0.001	-0.059
LPS	-89.162	14.292	-0.109	0.053	-0.056
SNG	100.620	7.173	0.005	-0.044	-0.039
ATL	-84.338	33.433	0.058	-0.093	-0.035
NIL	73.252	33.650	-0.069	0.059	-0.010
GEO	-77.067	38.900	-0.006	0.026	0.020
NAI	36.804	-1.274	-0.110	0.141	0.031
KOD	77.467	10.233	0.177	-0.138	0.039
STU	9.195	48.772	-0.001	0.041	0.040
SEO	126.967	37.567	-0.125	0.170	0.045
SHL	91.883	25.567	-0.081	0.126	0.045
AAE	38.766	9.029	-0.290	0.342	0.052
JCT	-99.802	30.479	0.095	-0.041	0.054
TRI	13.764	45.709	-0.193	0.247	0.054
SDB	13.572	-14.926	-0.049	0.109	0.060
LOR	3.851	47.267	0.008	0.081	0.089
FLO	-90.370	38.802	-0.100	0.195	0.095
DAL	-96.784	32.846	0.266	-0.164	0.102
MDS	-89.760	43.372	-0.091	0.202	0.111
KIP	-158.015	21.423	-0.041	0.180	0.139
EIL	34.950	29.550	-0.067	0.219	0.152

Table 4. Receiver and Path Effect on m_b of Novaya Zemlya Events					
Station	Lon	Lat	Rcv	Path	Rcv+Path
JER	35.197	31.772	-0.014	0.178	0.164
MAL	-4.411	36.728	-0.056	0.221	0.165
OXF	-89.409	34.512	0.169	-0.004	0.165
NDI	77.217	28.683	0.100	0.080	0.180
BAG	120.580	16.411	0.030	0.157	0.187
BLA	-80.421	37.211	0.022	0.173	0.195
VAL	-10.244	51.939	-0.024	0.227	0.203
MAN	121.077	14.662	0.367	-0.160	0.207
CAR	-66.928	10.507	0.209	0.012	0.221
TAB	46.327	38.068	0.290	-0.067	0.223
ATU	23.717	37.972	0.171	0.063	0.234
TRN	-61.403	10.649	0.140	0.108	0.248
PDA	-25.663	37.747	0.043	0.246	0.289
SHI	52.520	29.638	0.120	0.170	0.290
BUL	28.613	-20.143	-0.004	0.312	0.308
RCD	-103.208	44.075	0.334	0.008	0.342
AAM	-83.656	42.300	0.210	0.148	0.358
SHA	-88.143	30.694	0.396	-0.023	0.373
TOL	-4.049	39.881	0.120	0.300	0.420
BOZ	-111.633	45.600	0.046	0.442	0.488
ESK	-3.205	55.317	0.084	0.415	0.499
AQU	13.403	42.354	-0.102	0.602	0.500
IST	28.996	41.046	0.184	0.374	0.558
MSH	59.588	36.311	0.384	0.185	0.569
HLW	31.342	29.858	-0.256	0.836	0.580
COP	12.433	55.683	0.174	0.544	0.718

Figure 5 shows the scatter plot of 3 different types of station m_bs for Novaya Zemlya explosion 791018. The 39 good recordings, 7 noise, and 14 clips are shown with filled circles, Y-shaped downward arrows, and upward arrows, respectively. The raw station m_bs (top) have a standard deviation of 0.29 m.u. Applying the "primary" station corrections (cf. the "Rcv" column in Table 4; "S" term in [3]) reduces the scatter to 0.21 m.u. Applying the "secondary" corrections (cf. the "Path" column in Table 4; "F" term in [3]) to count for the propagation effects reduces the scatter further down to 0.11 m.u. The dashed lines of 1 σ range around the network-averaged m_b clearly illustrate the remarkable reduction of fluctuation across the recording stations. The mean event m_b itself is not significantly changed, however. Among 28 Novaya Zemlya events used in this study, this event has the smallest scatter in the resulting $m_{2.9}$ values. The dramatic reduction of variation from m_1 to $m_{2.9}$ shows a factor of nearly 2.7, as compared to the worst case of about 1.26 for the event 801011 (Figure 9). Novaya Zemlya events typically exhibit a reduction factor around 2 (e.g., Figure 7). Figure 6 shows the scatter plot of 3 different types of station m_bs for Novaya Zemlya explosion 780927. Among 28 Novaya Zemlya events used in this study, this event shows the most dramatic reduction of variation with a factor of 2.8.

Figures 8 and 9 are the same as Figure 5 except for the events 661027 and 801011, respectively. Although these two events do not show as dramatic reduction in variation as do other events, a factor of 1.4 still illustrates the robustness of our joint inversion scheme. The seismic disturbance of 801011 is known to be caused by two possibly simultaneous explosions of 7 km apart (Lilwall and Marshall, 1986; Stewart and Marshall, 1988). The resulting P-wave amplitude pattern is significantly different from the typical single shots from the same source region, which is why the station/path-correction procedure does not yield a performance as good as in other cases. Note that the path correction proposed in this study not only reduces the m_b scatter at stations that reported the good signals, but it also improves the data consistency of the censored recordings, as indicated by the shifting of the clipped recordings (e.g., Figures 5 and 6).

VARIOUS WWSSN MAGNITUDES OF EVENT 791018Z

Raw Station m_1's (No Correction Applied)

5.702 +/- 0.037 , σ= 0.289   39,7,14

Station $m_{2.2}$'s (Mean Receiver Effects Removed)

5.710 +/- 0.031 , σ= 0.239   39,7,14

Station $m_{2.9}$'s (Receiver & Path Terms Removed)

5.692 +/- 0.014 , σ= 0.108   39,7,14

Azimuth (degrees)
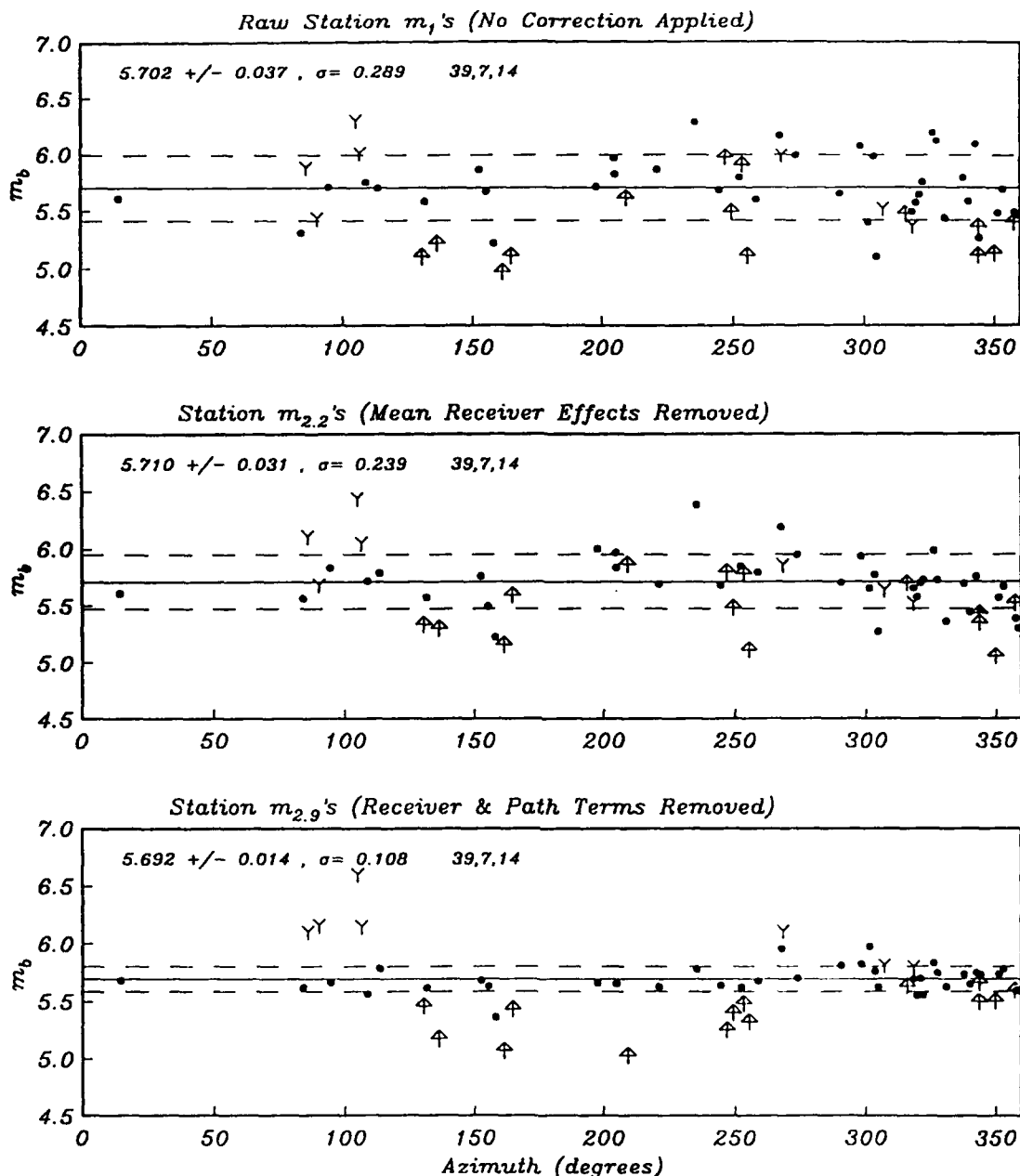
Figure 5. Scatter plot of 3 different types of station m_bs for Novaya Zemlya explosion 791018. The 39 good recordings, 7 noise, and 14 clips are shown with filled circles, Y-shaped downward arrows, and upward arrows, respectively. The raw station m_bs (top) have a standard deviation of 0.29 m.u. Applying the "primary" station corrections reduces the scatter to 0.21 m.u. Applying the proposed "secondary" corrections to count for the path effects reduces the scatter further down to 0.11 m.u. The dashed lines around the network-averaged m_b clearly illustrate the remarkable reduction of fluctuation across the recording stations. The mean event m_b itself is not significantly changed, however. Among 28 Novaya Zemlya events used in this study, this event has the smallest scatter in the resulting $m_{2.9}$ values. The dramatic reduction of variation from m_1 to $m_{2.9}$ shows a factor of nearly 2.7, as compared to the worst case of about 1.26 for the event 801011 (Figure 9). Novaya Zemlya events typically exhibit a reduction factor around 2.

VARIOUS WWSSN MAGNITUDES OF EVENT 780927Z

Raw Station m_1's (No Correction Applied)

5.506 +/- 0.042 , σ= 0.320   42,7,10

Station $m_{2.2}$'s (Mean Receiver Effects Removed)

5.546 +/- 0.037 , σ= 0.283   42,7,10

Station $m_{2.9}$'s (Receiver & Path Terms Removed)

5.519 +/- 0.015 , σ= 0.114   42,7,10

Azimuth (degrees)
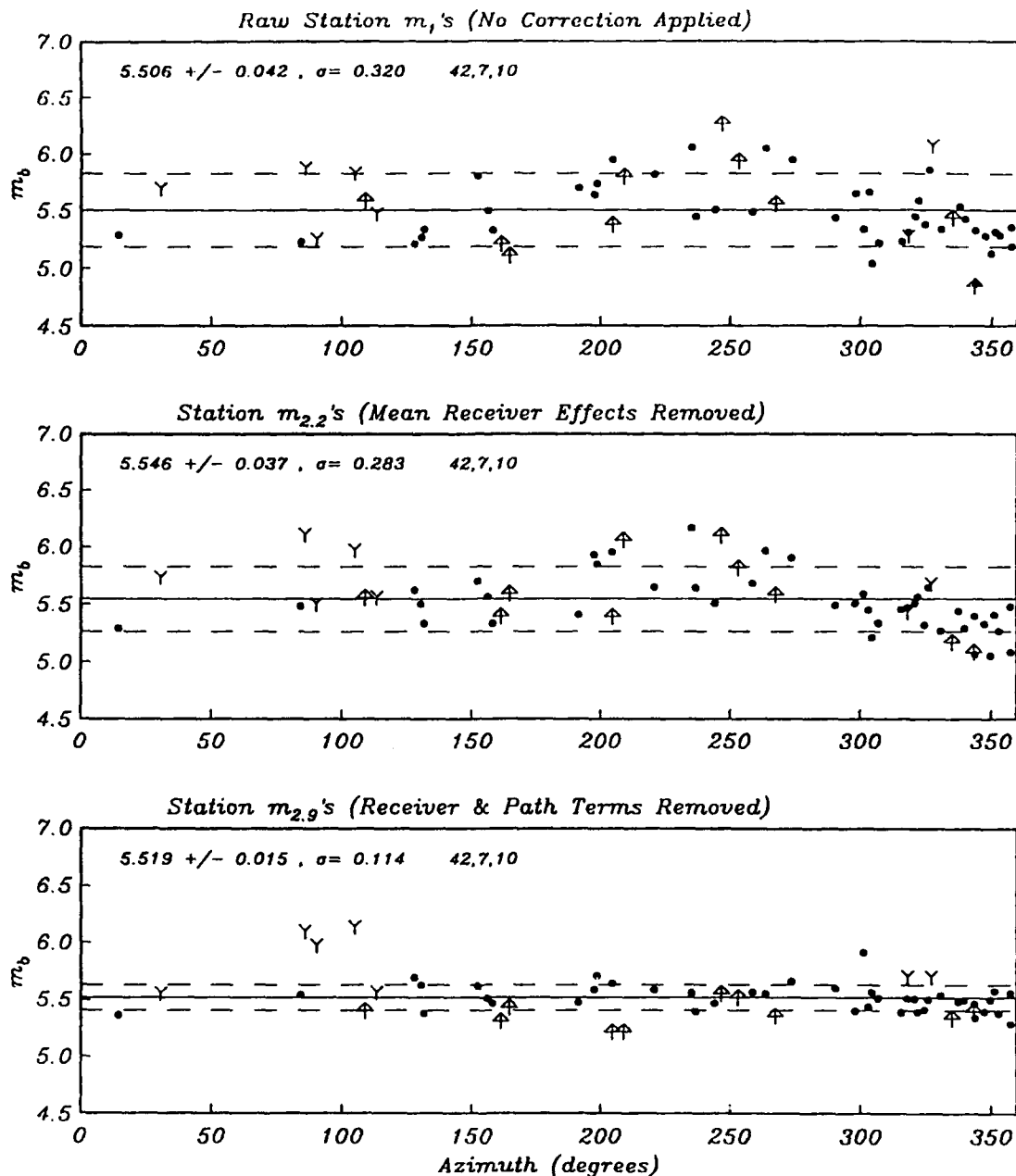
Figure 6. Scatter plot of 3 different types of station m_bs for Novaya Zemlya explosion 780927. Note that the raw station m_bs (top) have a standard deviation of 0.32 m.u., whereas the $m_{2.9}$ have a standard deviation of 0.11 m.u. Among 28 Novaya Zemlya events used in this study, this event shows the most dramatic reduction of variation with a factor of 2.8.

VARIOUS WWSSN MAGNITUDES OF EVENT 870802Z

Raw Station m_1's (No Correction Applied)

5.641 +/- 0.059 , σ= 0.330   22,3,6

Station $m_{2.2}$'s (Mean Receiver Effects Removed)

5.660 +/- 0.055 , σ= 0.304   22,3,6

Station $m_{2.9}$'s (Receiver & Path Terms Removed)

5.683 +/- 0.027 , σ= 0.150   22,3,6

Azimuth (degrees)
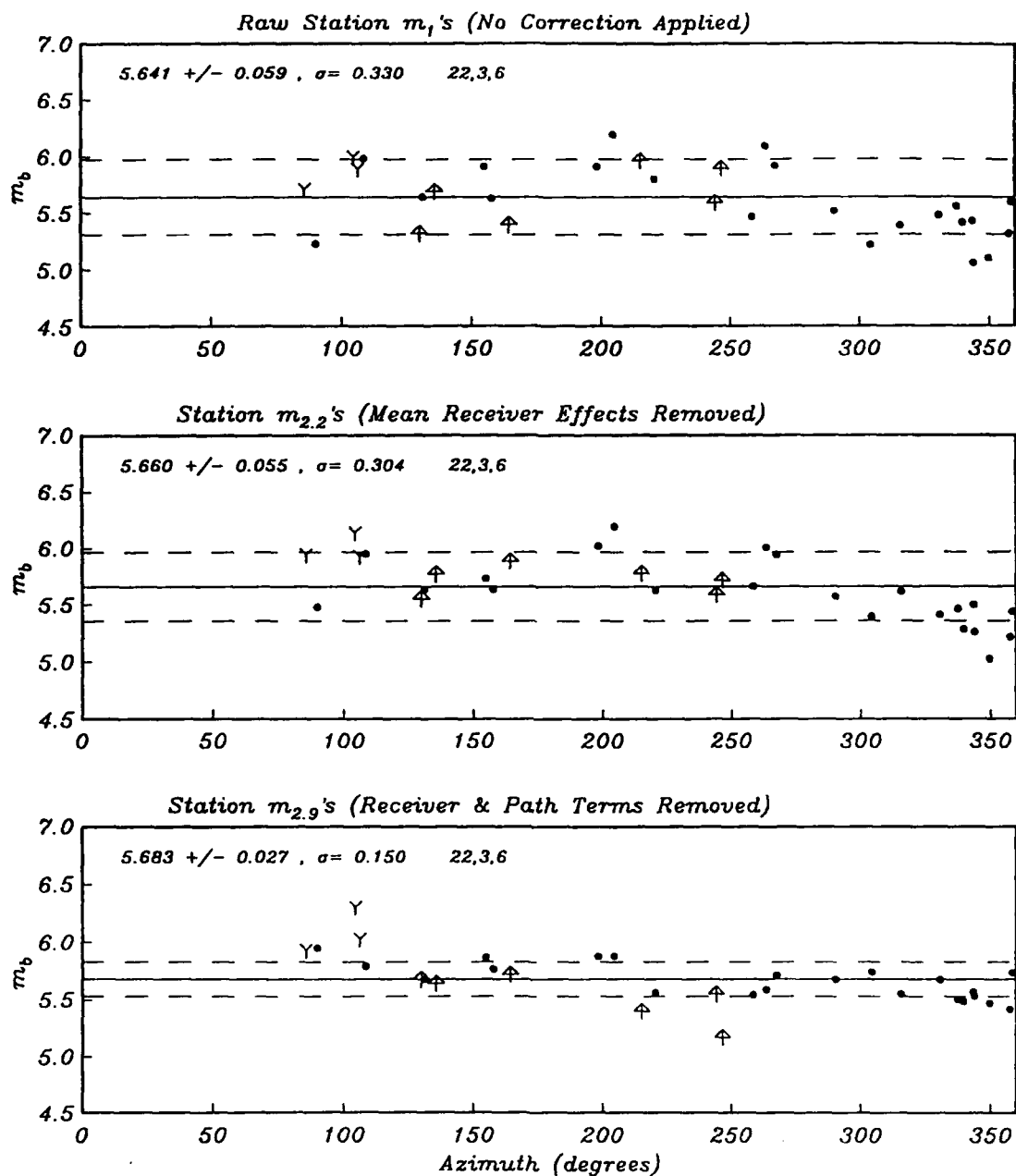
Figure 7. Same as Figure 5 except for the event 870802. The variation reduction with a factor of 2.2 is typical for Novaya Zemlya explosions.

Raw Station m_1's (No Correction Applied)

6.445 +/- 0.038 , σ= 0.312   56,0,13

Station $m_{2.2}$'s (Mean Receiver Effects Removed)

6.450 +/- 0.032 , σ= 0.267   56,0,13

Station $m_{2.9}$'s (Receiver & Path Terms Removed)

6.455 +/- 0.026 , σ= 0.220   56,0,13

Azimuth (degrees)
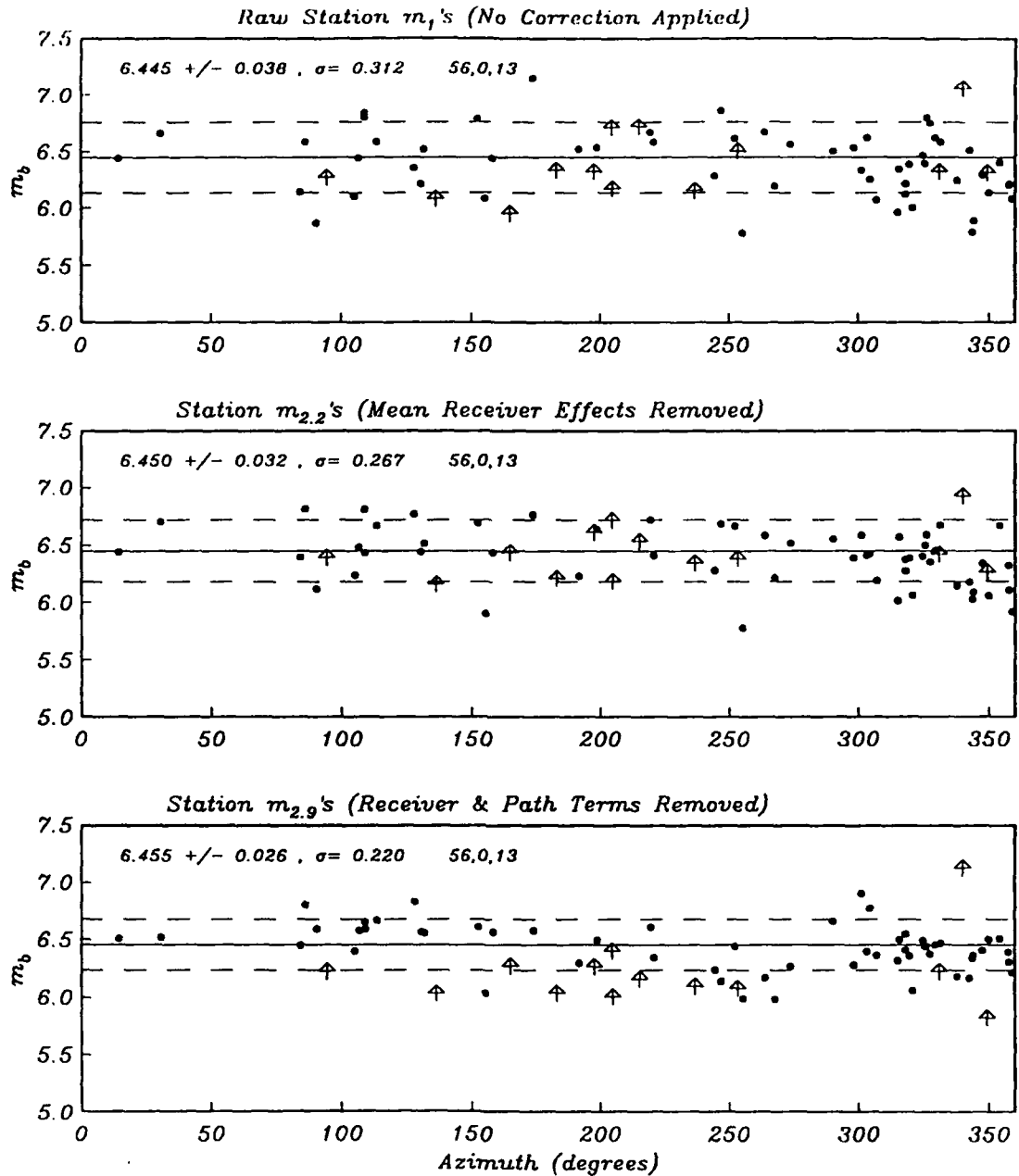
Figure 8. Same as Figure 5 except for the event 661027. Although this event does not show as dramatic reduction in variation as do other events, a factor of 1.4 still illustrates the robustness of our joint inversion scheme. Note that the path correction proposed in this study not only reduces the m_b scatter at stations that reported the good signals, but it also improves the data consistency of the censored recordings, as indicated by the shifting of the clipped recordings.

VARIOUS WWSSN MAGNITUDES OF EVENT 801011Z
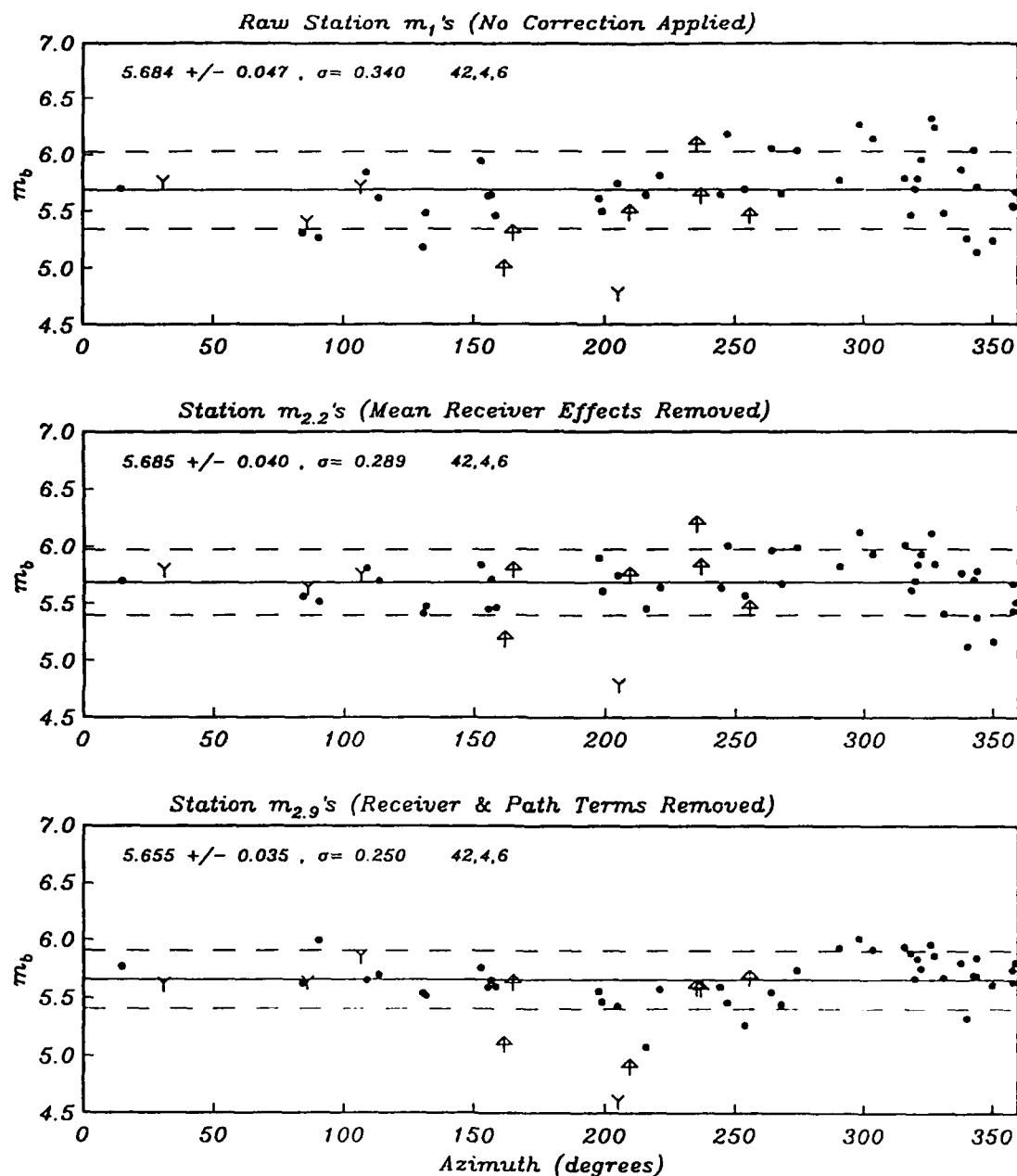
Figure 9. Same as Figure 5 except for the event 801011. This seismic disturbance is known to be caused by two possibly simultaneous explosions of 7 km apart (Lilwall and Marshall, 1986; Stewart and Marshall, 1988). The resulting P-wave amplitude pattern is significantly different from the typical single shots from the same source region, which explains why the station/path-correction procedure does not yield a performance as good as in other cases.

5. YIELD ESTIMATES OF NOVAYA ZEMLYA EXPLOSIONS

Without calibration shots, the absolute yields of Novaya Zemlya explosions would have to be estimated with some assumptions. Dahlman and Israelson (1977) used the announced yields of Soviet PNEs as the baseline. Burger et al. (1986) estimated the yields by assuming an average t^* and $\log(\Psi_\infty)$:yield scaling relation. The yield estimates from Sykes and Ruggi (1989) assume a m_b bias of 0.351 m.u. relative to NTS. Nuttli (1988) estimated the yields using his quadric equation (Nuttli, 1986a), which is based on the assumption that the L_g:yield relationship is transportable to NNZ without any correction.

In this section, we assume that the P_a scaling at Novaya Zemlya is about the same as that at Semipalatinsk. For events after 1976, the m_b:yield relationship at Matochkin Shar of Novaya Zemlya is solved with that at Semipalatinsk along with the yield-dependent P_{max}/P_a ratio at these two sites. For larger events (mainly detonated before TTBT became effective in 1976), we combine the theoretical $\log(\Psi_\infty)$:yield scaling in Bache (1982) and our m_b:$\log(\Psi_\infty)$ relationship using the relative source strengths determined by Burger et al. (1976).

A number of early studies appear to support the assumption of comparable coupling and mantle condition. Geologically, the rocks in the upper crust of Novaya Zemlya are of sedimentary origin, metamorphosed to lower greenschist facies, that may have physical properties similar to those of Soviet's Balapan test site (Leith et al., 1990). DARPA (1981, page 32) asserts that the mantle below Novaya Zemlya has significantly less attenuation as compared to the Basin and Range structure. Analysis of modern digital array data also favors a low t^* source region (Der et al., 1985).

Based on the published yields (Bocharov et al., 1989), the $m_b(P_a)$:yield relationship at KTS is:

$$m_b(P_a) = 0.802(\pm0.020) \log(W) + 3.834(\pm0.032) \qquad [6]$$

Regressing $m_b(P_{max})$ and $m_b(P_b)$ on $m_b(P_a)$ with NNZ events after 1976, we have:[1]

$$\text{NNZ: } m_b(P_b) = 1.055(\pm0.033) \, m_b(P_a) - 0.056(\pm0.171) \,, \quad \sigma = 0.045 \,, \quad \rho = 0.9926 \,. \qquad [7a]$$

$$\text{NNZ: } m_b(P_{max}) = 0.991(\pm0.033) \, m_b(P_a) + 0.446(\pm0.222) \,, \quad \sigma = 0.059 \,, \quad \rho = 0.9861 \,. \qquad [7b]$$

Under the assumption that NNZ and KTS have similar coupling and mantle condition (i.e., the

---

[1]For KTS events after 1976, $m_b(P_b)$ = 0.946(±0.025) $m_b(P_a)$ + 0.564(±0.131) (σ = 0.050, ρ = 0.9908), and $m_b(P_{max})$ = 0.923(±0.033) $m_b(P_a)$ + 0.912(±0.171) (σ = 0.065, ρ = 0.9839).

$m_b(P_a)$ scaling is transportable without any correction), the $m_b(P_b)$:yield relationship at NNZ can be determined with [1] and [2a] as:

$$\text{NNZ:} \quad m_b(P_b) = 0.846 \log(W) + 3.989 \qquad [8a]$$

Similarly, the $m_b(P_{max})$:yield relationship at NNZ can be determined with [6] and [7b] as

$$\text{NNZ:} \quad m_b(P_{max}) = 0.795 \log(W) + 4.245 \qquad [8b]$$

Table 5. Expected $m_{2.9}$ for Various Test Sites				
Phase/site	1 KT	10 KT	50 KT	100 KT
$m_b(P_{max})$ (NNZ)	4.245	5.040	5.596	5.835
$m_b(P_{max})$ (KTS)	4.399	5.167	5.704	5.935
$m_b(P_{max})$ (NTS)	3.954	4.771	5.342	5.588
$m_b(P_b)$ (NNZ)	3.989	4.835	5.426	5.681
$m_b(P_b)$ (KTS)	4.130	4.930	5.489	5.730
$m_b(P_b)$ (NTS)	3.674	4.505	5.086	5.336
$m_b(P_a)$ (KTS,NNZ)	3.834	4.636	5.197	5.438
$m_b(P_a)$ (NTS)	3.607	4.372	4.907	5.137

Table 5 lists the expected m_b values for each of P_a, P_b, and P_{max} phases from NTS, NNZ, and KTS explosions based on Equations [6] and [8]. The estimated "mean" $m_{2.9}$ bias can then be computed in a straightforward manner (Table 6). The bias estimates based on $m_{2.2}$ can be found in Jih and Wagner (1991b). Leith et al. (1990) suggest that the NNZ explosions are primarily emplaced in near-horizontal tunnels, excavated into the steep mountain slopes. Thus it would seem plausible that the difference in the free-surface interaction at NNZ and Balapan/Murzhik could contribute much of the m_b bias in P_{max} and P_b we are observing. The majority of NNZ explosions after 1976 are clustered at yields between 50 and 70 KT (cf. Table 8). Within this range of yield, the expected m_b bias is about -0.11 m.u. relative to KTS using $m_b(P_{max})$, which can explain satisfactorily why Evernden and Marsh (1987) and Sykes and Cifuentes (1984) observe the same m_b bias of about 0.1 m.u. between Semi-palatinsk and Novaya Zemlya on their M_S:m_b plot.

Table 6. Mean $m_{2.9}$ Bias				
Phase	1 KT	10 KT	50 KT	100 KT
$m_b(P_{max})$ (KTS-NTS)	0.45	0.40	0.36	0.35
$m_b(P_b)$ (KTS-NTS)	0.46	0.43	0.40	0.39
$m_b(P_a)$ (KTS-NTS)	0.23	0.26	0.29	0.30
$m_b(P_{max})$ (NNZ-NTS)	0.29	0.27	0.25	0.25
$m_b(P_b)$ (NNZ-NTS)	0.32	0.33	0.34	0.35
$m_b(P_a)$ (NNZ-NTS)	0.23	0.26	0.29	0.30

Burger *et al.* (1986) estimated the relative source strengths of 11 NNZ events detonated before 1976 based on the intercorrelation method with the event 671021 as a reference (Table 7). Regressing our path-corrected m_b values on these relative source strengths, we have:

$$m_b(P_a) = 0.854(\pm 0.048) \ \log[\Psi_\infty/\Psi_\infty(671021)] + 5.472(\pm 0.032) \qquad [9a]$$

$$m_b(P_b) = 0.900(\pm 0.048) \ \log[\Psi_\infty/\Psi_\infty(671021)] + 5.672(\pm 0.033) \qquad [9b]$$

$$m_b(P_{max}) = 0.856(\pm 0.047) \ \log[\Psi_\infty/\Psi_\infty(671021)] + 5.856(\pm 0.032) \qquad [9c]$$

Table 7. Relative Source Size $\Psi_\infty/\Psi_\infty(671021)$ of Novaya Zemlya Explosions[*]		
Event	$\Psi_\infty/\Psi_\infty(671021)$	S.E.M.
661027	5.26	0.43
671021	1.00	0.11
681107	1.53	0.12
691014	2.22	0.16
701014	11.29	1.01
710927	7.47	0.66
720828	4.10	0.36
730912	16.24	2.20
740829	5.44	0.48
750823	5.28	0.45
751021	4.96	0.56

[*]: from Burger *et al.*, (1986).

In deriving Equation [9], the standard errors in both m_b and Ψ_∞ measurements (shown in Tables 1 and 7, respectively) are taken into account using a generalized regression procedure described in Jih and Wagner (1991b) and Jih *et al.* (1991). Combining the theoretical $\log(\Psi_\infty)$:yield scaling of $\log(\Psi_\infty) = 0.89 \log(W) + C$ (*e.g.*, Bache, 1982), we can infer the m_b:yield relationship for larger Novaya Zemlya explosions as

$$m_b(P_a) = 0.760 \log(W) + 3.920 \qquad [10a]$$

$$m_b(P_b) = 0.801 \log(W) + 4.079 \qquad [10b]$$

$$m_b(P_{max}) = 0.762 \log(W) + 4.312 \qquad [10c]$$

Equation [10a] is used if $m_b(P_a)$ is larger than 5.472. Similar turning points for $m_b(P_b)$ and $m_b(P_{max})$ are set at 5.672 and 5.856, respectively, which are the corresponding intercepts in Equations [9a] through [9c]. At these turning points, Equations [8] and [10] give identical result, as we have used these turning points to constraint the unknown constant C in the theoretical $\log(\Psi_\infty)$ scaling.

Figures 10 through 12 show the regression of $m_{2.9}(P_a)$, $m_{2.9}(P_b)$, and $m_{c.9}(P_{max})$ on the relative source size $\Psi_\infty/\Psi_\infty(671021)$ determined by Burger *et al.* (1986), which correspond to

Equations [9a] through [9c], respectively. The uncertainties in the m_bs and the $\Psi_\infty/\Psi_\infty(671021)$ are taken into account through 800 bootstrap resamplings. The darkened bundle is actually the collection of all 800 regressions, each produced by a possible realization of 11 perturbed $(m_b, \Psi_\infty/\Psi_\infty(671021))$ pairs. The 95% confidence band (shown as 2 curves around the darkened bundle) is narrower near the centroid and wider towards both ends, as expected. The individual 95% confidence intervals of the two inferred parameters (*i.e.*, the slope and the intercept of the calibration curve) are shown with the dashed line in the scatter plot (bottom). Note that the dashed rectangle is not the joint 90% confidence interval, however, due to the highly correlated nature of the two parameters. The P_b phase appears to fit the relative source sizes slightly better than do P_a and P_{max}.

Table 8 gives our yield estimates based on the $m_{2.9}$ measurements listed in Table 1. For comparison, the yields estimated by Nuttli (1988), Sykes and Ruggi (1989), and Burger *et al.* (1986) are also included. Most of Nuttli's (1988) yield estimates based on his quadric formula tend to be larger, as noted by Lay (1991). Sykes and his colleagues (Sykes and Wiggins, 1986; Sykes and Davis, 1987; Sykes and Ruggi, 1989) examined the apparent clustering of certain yields of Novaya Zemlya explosions in the context of particular warhead types, and they estimated the peak value as 500 and 90 KT for events before and after 1976, respectively. Our peak value for recent events lies between Sykes' 90 KT and Israelson's (1991) 50 KT. To lower down our estimate of the peak value would imply that NNZ has basic coupling much more efficient than that at KTS or that NNZ has a less attenuating mantle than KTS, which would seem unlikely. Therefore Israelson's (1991) peak value of 50 KT could be somewhat low. Recent laboratory experiments by Miller and Florence (1991) indicate that saturated limestones under the frozen condition could have a poorer coupling. Thus there is a possibility that yield estimates of Novaya Zemlya events based on *every* seismic method could be slightly underestimated, and *all* the peak values might need be increased somewhat (Blandford, personal communication).

There is a clustering of four NNZ events around $\Psi_\infty/\Psi_\infty(671021) = 5.235$ before 1976 (Figures 10 through 12), which corresponds to 577, 510, and 556 KT in Equations [10a], [10b], and [10c], respectively. Between 1973 and 1976 the U.S.S.R. deployed five strategic systems with warhead yields between 300 and 600KT according to some non-seismic source of information (Samuel, 1985; Sykes, 1985; Evernden and Marsh, 1987), which provides an indirect support of our estimate of 550KT and Sykes' 500KT for the repeated tests at NNZ prior to TTBT era.

mb:Yield Relationship at Novaya Zemlya

mb(WWSSN,ML8,Pa)

PSI/PSI(ref) (Burger et al., 1986)
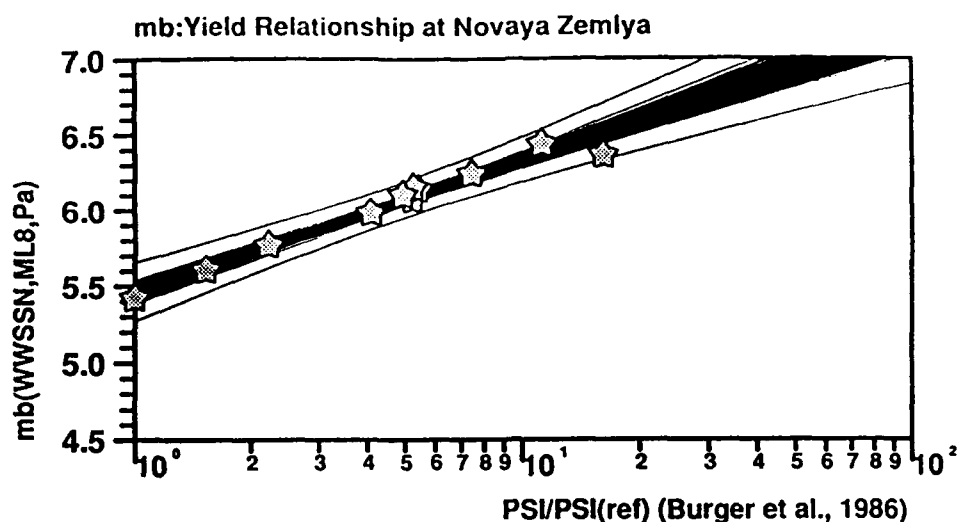
DWLS (uncertain X & Y): S=0.85(0.048), I=5.47(0.032), 11. data used,
95% error in Y at X=1,5,10,50,100:   0.18, 0.12, 0.15, 0.32, 0.40,
95% factor in X at X=1,5,10,50,100:   2.69, 1.94, 2.29, 5.67, 8.70

OWLS (precise X assumed): S=0.87(0.051), I=5.46(0.036)

Standard LS: S=0.86(0.056), I=5.47(0.041)

Scatter Plot of Inferred Parameters

800-bootstrap Intercepts

800-bootstrap Slopes
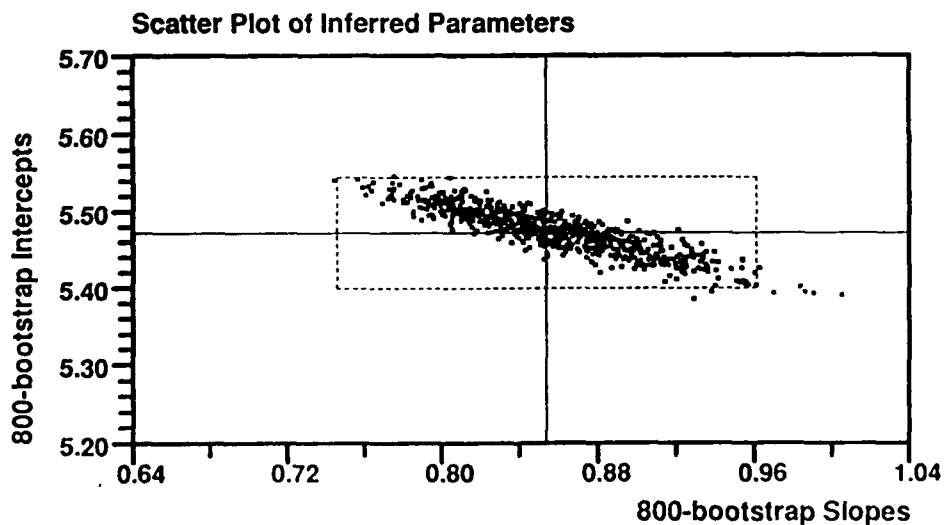
95% confidence interval of slope: 0.85+/-0.108
95% confidence interval of intercept: 5.47+/-0.073
[97.5% quantile of t(9. D.o.F.), 2.262, used]

Figure 10. Regressing the $\overline{m}_{2.9}(P_a)$ on the relative source size $\Psi_\infty/\Psi_\infty(671021)$ determined by Burger et al. (1986). The uncertainties in the m_bs and the $\Psi_\infty/\Psi_\infty(671021)$ are taken into account through 800 bootstrap resamplings. The darkened bundle is actually the collection of all 800 regressions, each produced by a possible realization of 11 perturbed (m_b, $\Psi_\infty/\Psi_\infty(671021)$) pairs. The 95% confidence band (shown as 2 curves around the darkened bundle) is narrower near the centroid and wider towards both ends, as expected. The individual 95% confidence intervals of the two inferred parameters (i.e., the slope and the intercept of the calibration curve) are shown with the dashed line in the scatter plot (bottom). Note that the dashed rectangle is not the joint 90% confidence interval, however, due to the highly correlated nature of the two parameters.

- 32 -

mb:Yield Relationship at Novaya Zemlya

PSI/PSI(ref) (Burger et al., 1986)

DWLS (uncertain X & Y): S=0.90(0.048), I=5.67(0.033), 11. data used,
95% error in Y at X=1,5,10,50,100: 0.17, 0.12, 0.14, 0.29, 0.36,
95% factor in X at X=1,5,10,50,100: 2.37, 1.83, 2.05, 4.46, 6.37

OWLS (precise X assumed): S=0.91(0.038), I=5.66(0.027)

Standard LS: S=0.91(0.042), I=5.67(0.031)

Scatter Plot of Inferred Parameters

800-bootstrap Slopes

95% confidence interval of slope: 0.90+/-0.108
95% confidence interval of intercept: 5.67+/-0.074
[97.5% quantile of t(9. D.o.F.), 2.262, used]

Figure 11. Same as Figure 10 except that $m_{2.9}(P_b)$ are used. The P_b phase appears to fit the relative source sizes slightly better than do P_a and P_{max}.

mb:Yield Relationship at Novaya Zemlya

Scatter Plot of Inferred Parameters
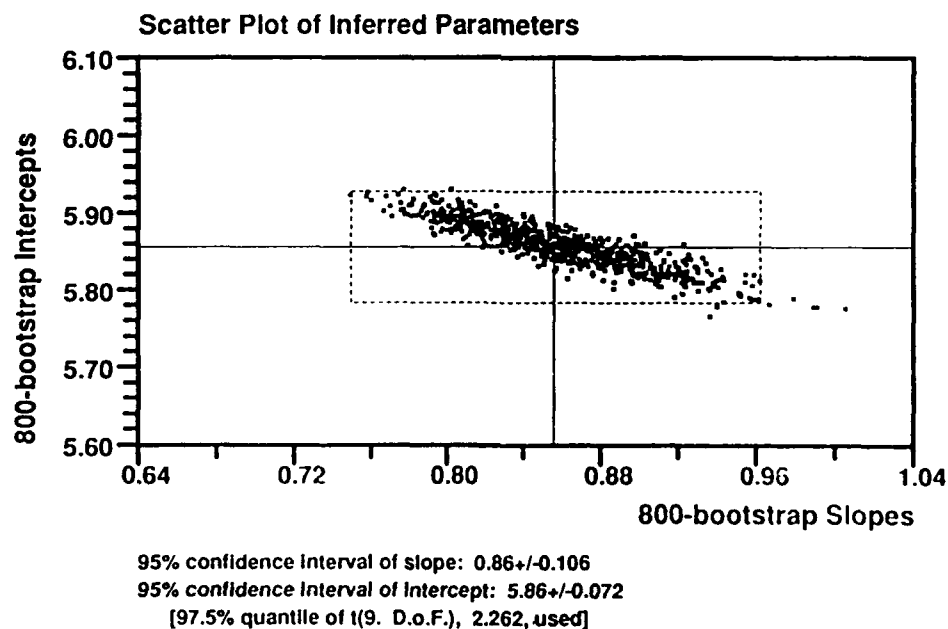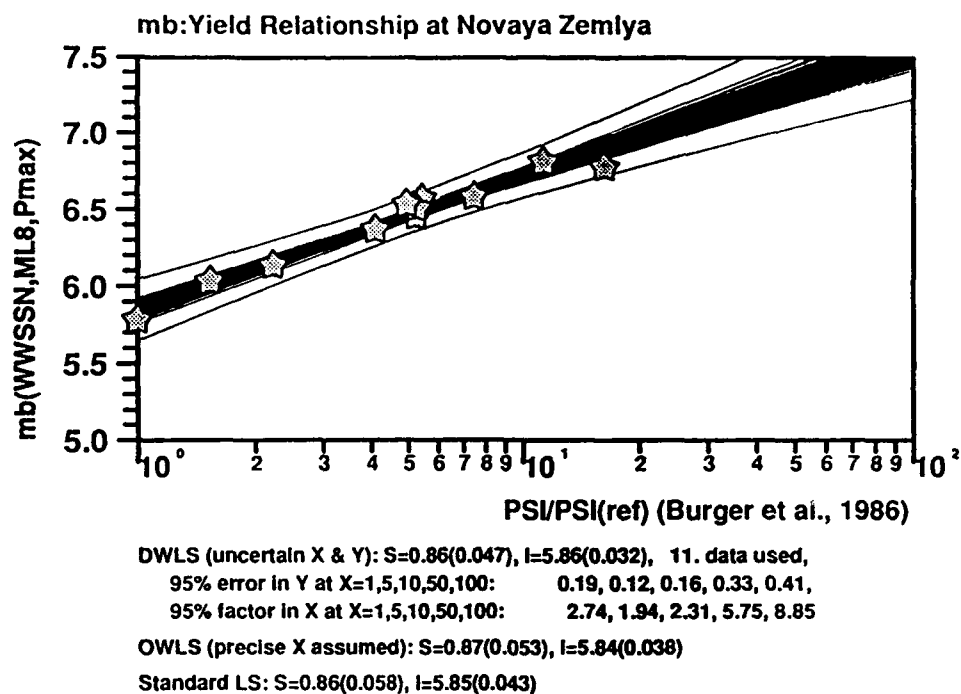
Figure 12. Same as Figure 10 except the $m_{2.9}(P_{max})$ are used.

Table 8. Yield Estimates of Novaya Zemlya Explosions						
Event	Yield [KT] (this study)			Yield [KT] (earlier study)		
Date	P_a	P_b	P_{max}	SR[1]	$m_b(L_g)$[2]	BBL[3]
661027	673	602	642	422	644	600
671021	96	82	86	93	180	61
681107	164	161	180	119	253	110
691014	270	225	245	140	399	183
701014	2058	1537	1888	1001	1970	1714
710927	1140	893	945	586	1500	973
720828	518	488	498	329	580	426
730912	1639	1764	1693	2099	3510	2824
740829	834	760	917	497	1110	629
750823	862	766	760	477	690	604
751021	748	647	820	497	600	554
760929	58	56	51	70	91	—
761020	3	4	5	13	19	—
770901	46	55	50	55	122	—
771009	3	2	2	4	10	—
780810	93	89	109	89	91	—
780927	38	42	41	44	61	—
790924	66	71	76	55	81	—
791018	68	61	67	70	79	—
801011	49	52	61	55	76	—
811001	63	63	63	113	116	—
821011	40	35	32	44	79	—
830818	70	65	69	89	145	—
830925	58	56	57	70	99	—
841025	49	55	54	89	—	—
870802	71	66	65	70	—	—
880507	42	37	34	—	—	—
881204	63	70	63	—	—	—

1: from Sykes and Ruggi (1989); based on body-wave magnitudes.

2: from Nuttli (1988); based on the quadric fit.

3: from Burger et al. (1986); based on Amchitka scaling.

5. YIELD ESTIMATES WITH NUTTLI'S L_g MEASUREMENTS

Lay (1991) suggests that there still exists significant uncertainty in yield estimates for many of the early large events at Novaya Zemlya. We note that Nuttli's (1988) yield estimates are systematically larger than those inferred by Burger *et al.* (1986), while our yield estimates for the larger historical events seem to lie between these two (with 730912 as an exception; *cf.* Table 10). A few experiments with Nuttli's (1988) $m_b(L_g)$ measurements have been conducted to explore some of the possibilities.

The first question to be examined is whether Nuttli's (1986a) L_g scaling formulae are adequate. Jih *et al.* (1990) point out that it is not quite clear how Nuttli's (1986a) derived his original linear calibration formula. Nuttli's data set of high-coupling NTS shots (*cf.* Nuttli, 1986a, page 2144) included the Pahute Mesa event HANDLEY which has an announced yield of >1000KT. However, Nuttli seemed to have treated the yield as exactly 1000KT in his calculations (*cf.* Figures 7 and 9 of Nuttli, 1986a). Jih *et al.* (1990) tested eight possible combinations with Nuttli's $m_b(L_g)$ measurements:

- including the granite events (SHOAL and PILEDRIVER) or not,

- limiting $m_b(L_g)$ to [5.2,6.7] or not,

- assuming HANDLEY was 1000KT or deleting HANDLEY from the regression.

None of the eight experiments could give an exactly identical formula to the linear fit given by Nuttli (1986a). It seems very likely that Nuttli might have regressed the published yields on his $m_b(L_g)$ values (*i.e.*, the so-called "Y-regression" models) with some unspecified constraint on the data set.

A more extensive data set of NTS $m_b(L_g)$ values has been compiled by R. Geil at Lawrence Livermore National Laboratory [LLNL] (Patton, 1988). This data set consists of 47 events below the water table on Pahute Mesa and Yucca Flat of NTS. Patton (1988) regressed this data set against the official yields, and the calibration curve meets that of Nuttli's (1986a) at $m_b(L_g)$=6.028 or 178KT. Beyond that level, yield estimates based on Geil's data set are even larger than that by Nuttli (1986a). Patton (1988) repeated Nuttli's (1986a) procedure to estimate the yields of 69 NTS high-coupling shots using *RMS* L_g magnitudes measured at LLNL's high-quality regional digital network. The resulting scaling curve is nearly parallel to that of Nuttli's, and hence yield estimates based on Patton's formula are systematically smaller than those with Nuttli's or Geil's results (Tables 9 and 10). For instance, based on Patton's regression result, the predicted $m_b(L_g)$ at explosive yields of 10, 50, 100, 150KT

are 5.159, 5.687, 5.914, and 6.047, respectively. Nuttli's (1986a) original regression with 22 NTS shots recorded at WWSSN stations gives 5.072, 5.607, 5.837, and 5.972, respectively. The NTS explosions Patton used are clustered around $m_b(L_g) \approx 5.8$. Beyond that level, the difference in yield estimates between Nuttli's and Patton's predictions are by no means negligible. The data recorded at LLNL's regional digital network probably have a quality better than those WWSSN film chips which Nuttli (1986a) read. Perhaps it is reasonable to expect that the Patton's (1988) $m_b(L_g)$:yield calibration curve is more accurate than Nuttli's. Table 9 gives the predicted yield at several $m_b(L_g)$ levels, with the applicable range of each scaling formula ignored.

Table 9. Expected Yields [KT] at Given $m_b(L_g)$ Values					
Scaling	4.5	5.0	5.5	6.0	6.5
Nuttli(1986a)[1]	3	10	37	152	779
Nuttli(1986a)[2]	2*	8*	36	163	736
Geil[3]	1*	5*	29	162	885
Patton(1988)[4]	1	6	28	130	597

1) Nuttli's (1986a) quadric formula: $m_b(L_g) = 3.943 + 1.124 \log(W) - 0.0829 [\log(W)]^2$.

2) Nuttli (1986a): $m_b(L_g) = 4.307 [\pm 0.067] + 0.765 [\pm 0.027]\log(W)$ for $5.2 < m_b(L_g) < 6.7$.

3) Geil (Patton, 1988): $m_b(L_g) = 4.505 [\pm 0.067] + 0.677 [\pm 0.029]\log(W)$ for $5.28 < m_b(L_g) < 6.65$.

4) Patton (1988): $m_b(L_g) = 4.404 [\pm 0.048] + 0.755 [\pm 0.022]\log(W)$ for $4.22 < m_b(L_g) < 6.7$.

*) Extrapolated value.

Table 10 gives the yield estimate of NNZ events inferred from Nuttli's (1988) $m_b(L_g)$ values and various L_g scaling relationship, assuming that these L_g scaling formulae are portable and that Nuttli's $m_b(L_g)$ measurements of NNZ events are accurate. In comparing Table 8 against 10, we do see some indication that substituting Nuttli's (1988) NNZ $m_b(L_g)$ values into Patton's (1988) L_g scaling for NTS shots could give yield estimates in better agreement with our yields, particularly with those based on the P_b phase. However, further investigation is definitely necessary.

Table 10. Yield Estimates Based on Nuttli's $m_b(L_g)$ Measurements						
Event		Yield [KT]				
Date	$m_b(L_g)$	Nuttli[1]	Nuttli[2]	Nuttli[3]	Geil[4]	Patton[5]
640918	4.37	2.5	2	1*	1*	1
641025	5.19	16.4	17	14	10*	11
661027	6.45	644	653	633	746	513
671021	6.06	180	182	196	198	156
681107	6.17	253	257	272	288	218
691014	6.31	399	405	415	464	335
701014	6.75	1970	2000	1561	2071	1280
710927	6.68	1500	1519	1265	1632	1034
720828	6.42	580	588	578	674	468
730912	6.89	3510	3572	2379*	3333*	1962*
740829	6.60	1110	1122	994	1243	810
750823	6.47	690	700	672	799	545
751021	6.43	600	609	596	697	482
760929	5.83	91	92	98	91	77
761020	5.24	19	19	17	12*	13
770901	5.93	122	123	132	127	105
771009	4.99	10	10	8	5	6
780810	5.83	91	92	98	91	77
780927	5.69	61	62	64	56	51
790924	5.79	81	82	87	79	69
791018	5.78	79	80	84	76	66
801011	5.77	76	77	82	74	64
811001	5.91	116	116	125	119	99
821011	5.78	79	80	84	76	66
830818	5.99	145	147	158	156	126
830925	5.86	99	100	107	100	85

1) Nuttli-furnished yields based on his quadric formula (page 881 of Nuttli, 1988).

2) Recomputed estimates with Nuttli's (1986a) quadric formula (see footnote of Table 9).

3) Nuttli's (1986a) linear fit (see footnote of Table 9).

4) Geil (Patton, 1988) (see footnote of Table 9).

5) Patton (1988) (see footnote of Table 9).

*) Extrapolated value.

Lay (1991) compared a megaton-level Amchitka event MILROW with two Novaya Zemlya events of comparable M_S,[2] and asserts that there is significant discrepancy in the yield estimates based on body wave and surface wave. We feel a little more optimistic on this issue, if the uncertainty in each estimate is taken into account. Table 11 lists our $m_{2.9}$ of these two NNZ events (from Table 1) and MILROW (Jih and Wagner, 1992). The yield estimates of Burger et al. (1986) are in reasonable agreement with our estimate based on P_a (or P_b, P_{max}; cf. Table 8). Nuttli's (1988) $m_b(L_g)$ measurements simply suggest these two NNZ events could have very comparable size in terms of L_g excitation alone.

Table 11. Comparison of MILROW and 2 Novaya Zemlya Explosions							
Event	$m_{2.9}$ (this study)			Yield Estimate			
	$m_b(P_{max})$	$m_b(P_b)$	$m_b(P_a)$	P_a	BBL	Geil	Patton
MILROW	6.618	6.321	6.071	—	—	—	—
701014	6.808	6.631	6.438	2058	1714	2071	1280
710927	6.579	6.442	6.243	1140	973	1632	1034

---

[2]Marshall et al. (1979) and Douglas et al. (1987) give M_S of MILROW as 5.05 and 5.2, respectively. Sykes and Ruggi (1989) estimate the M_S of 701014Z and 710927Z as 5.02 and 5.06, respectively.

6. CONCLUSIONS AND RECOMMENDATIONS

Along with an extensive data set of worldwide explosions recorded at a global network, teleseismic body-wave amplitudes from 28 Novaya Zemlya explosions are measured and analyzed to isolate the propagation characteristics and to derive a better measure of the source size. This new m_b factoring procedure provides more stable m_b measurements across the whole recording network with a reduction in the fluctuational variation by a factor of up to 3. The variation reduction is typically a factor of 2, except for a known double explosion which has a factor of 1.26. In principle, this procedure can be applied to other types of network-recorded magnitudes as well, such as $\hat{m}_b$ (the band-passed spectral amplitude, see Bache, 1982, and Murphy et al., 1989), $m_b(L_g)$, M_o, and M_S.

Our result indicates that paths from the northern test site in Novaya Zemlya to stations in North America have systematically faster arrivals and smaller amplitudes, suggesting a profound defocusing effect on the first arrivals; while stations in Ireland, Scotland, Spain, Bangladesh, northern India, Pakistan, Korea, and Kenya report slow arrivals and large amplitudes, suggesting a focusing effect. Amplitudes for paths to Greenland, Iceland, Alaska, Turkey, Germany, Luzon, Zimbabwe, Italy, Pueto Rico, Ethiopia, and Hawaii, however, seem to be controlled by the anelastic attenuation with slow rays also associated with small amplitudes, and fast rays associated with large amplitudes. For paths showing strong attenuation or strong defocusing, our observations favor the "weak signal" hypothesis which predicts complex waveforms for such paths. The separation of path effects from station effects also provides direct clues as how an old fold-belt structures (like Novaya Zemlya) could "modulate" the short-period P–wave amplitude and the travel-time patterns, in a manner similar to that tectonic release affects M_S. A strong correlation between P–wave amplitude and L_g detection at teleseismic distance is also observed. Thus a thorough assessment of WWSSN's remote monitoring capability along this line could provide useful clues such as which stations should be searched for the L_g phase. Naturally, such "detection map" will be varying from one test site to another, as discussed in Jih and Wagner (1992).

Although our results can explain some of the propagation complexities in the initial P–wave arrivals, a follow-up study is needed to quantify further the contribution of near-source scattering to the waveform complexity in the P coda (such as that in Lay and Welc, 1987) which is not covered in this study. Our previous modeling effort (McLaughlin and Jih, 1986, 1987, 1988; Jih and McLaughlin, 1988) of utilizing the linear finite-difference code (Jih et al., 1988) focused on the effects of mountainous topography and hypothetical

heterogeneity in the upper crust on teleseismic and regional phases with somewhat simplied structures of other test sites. We suggest that the follow-up research be accompanied with some well-constrained forward modeling study using more realistic structures of Novaya Zemlya.

Assuming the basic coupling and the mantle condition at Novaya Zemlya are comparable to those at Eastern Kazakhstan, the yield estimates for the 28 Novaya Zemlya events based on the path-corrected m_b presented in this study range from 2 to 2100 KT, with peak values at 550KT and 65KT for events before and after 1976, respectively. The relative source size determined by Burger *et al.* (1986) and the theoretical Ψ_∞:yield scaling are combined to extrapolate the m_b scaling to higher end, and the resulting yield estimates are in reasonable agreement with those in previous studies.

There appears to be a bias of 0.11 magnitude units in $m_b(P_{max})-m_b(P_a)$ between Eastern Kazakh and Novaya Zemlya. This bias could be largely due to the difference in pP interference at these two test sites. Previous studies suggest a m_b bias of about 0.35 m.u. between NNZ and NTS, based on the spectral slope study (*e.g.*, Der *et al.*, 1985) and the m_b:M_S shift (*e.g.*, Evernden and Marsh, 1987). Result presented in this study gives a $m_b(P_{max})$ bias of about 0.25 m.u. (NNZ-NTS) and 0.36 m.u. (KTS-NTS) at 50 KT level. It seems that Nuttli's (1988) Balapan-NNZ bias (relative to $m_b(L_g)$) may be slightly biased high by about 0.05 m.u., which is very likely to be resulted from the inherent inconsistency associated with the ISC bulletin m_b values that Nuttli (1986b, 1987, 1988) used. Note that ISC bulletin m_b is just the simple network average of the raw station m_b (*i.e.* m_1 in Equation [1]) values without any further processing. Our study illustrates the advantages and importance of adopting some sophisticated post-processing methodology in determining the optimal network m_b values, even when the network (such as WWSSN and ISC) already possess a broad spatial coverage.

7. ACKNOWLEDGEMENTS

8. REFERENCES

Bache, T. C. (1982). Estimating the yield of underground nuclear explosions, *Bull. Seism. Soc. Am.*, **72-6**, S131-168.

Baumgardt, D. R. (1985). Comparative analysis of teleseismic P coda and L_g waves from underground nuclear explosions in Euroasia, *Bull. Seism. Soc. Am.*, **75**, 1413-1433.

Baumgardt, D. R. (1991). High frequency array studies of long range L_g propagation and the causes of L_g blockage and attenuation in the Eurasian continental craton, *Report PL-TR-91-2059(I)*, Phillips Laboratory, Hanscom Air Force base, MA. ADA239201

Blandford, R. R. and R. H. Shumway (1982). Magnitude:yield for nuclear explosions in granite at the Nevada Test Site and Algeria: joint determination with station effects and with data containing clipped and low-amplitude signals, *Report VSC-TR-82-12*, Teledyne Geotech, Alexandria, Virginia.

Bocharov, V. S., S. A. Zelentsoz, and V. Mikhailov (1989). Characteristics of 96 underground nuclear explosions at the Semipalatinsk test site, *Atomic Energy*, **67**, 210-214

Bonham, S., W. J. Dempsey, J. Rachlin (1980). Geologic environment of the Semipalatinsk area, U.S.S.R. *(Preliminary Report)*, U.S. Geological Survey, Reston, VA 22092.

Booth, D. C., P. D. Marshall, and J. B. Young (1974). Long and short period P-wave amplitudes from earthquakes in the range 0°-114°, *Geophys. J.*, **39**, 523-537.

Burdick, L. J. (1981). The changing results on attenuation of P waves, in *"A technical assessment of seismic yield estimation"*, *Report DARPA-NMR-81-01, Appendix*, DARPA, Arlington, VA.

Burger, R. W., L. J. Burdick, and T. Lay (1986). Estimating the relative yields of Novaya Zemlya tests by waveforms intercorrelation, *Geophys. J. R. astr. Soc.*, **87**, 775-800.

Butler, R. (1981). Estimation of body wave magnitudes and site specific propagation effects, in *"A technical assessment of seismic yield estimation"*, Report DARPA-NMR-81-01, Appendix, DARPA, Arlington, VA.

Butler, R. and L. Ruff (1980). Teleseismic short-period amplitudes: source and receiver variations, *Bull. Seism. Soc. Am.*, **70-3**, 831-850.

Chan, W. W. and B. J. Mitchell (1985). Surface wave dispersion, crustal structure and sediment thickness variations across the Barents Shelf, *Geophys J. R. Astron. Soc.*, **80**, 329-344.

Chan, W. W., I. S. Sacks and R. J. Morrow (1989). Anelasticity of the Iceland Plateau region from broad-band surface wave studies, *J. Geophy. Res.*, **94**, 5675-5688.

DARPA (1981). A technical assessment of seismic yield estimation, Report DARPA-NMR-81-02, DARPA/NMRO, Arlington, VA.

Dahlman, O. and H. Israelson (1977). *Monitoring Underground Nuclear Explosions*, Elsevier Scientific Publishing Co., New York.

Davies, D. (1970). Some remarks on short period discrimination, paper presented at *Woods Hole Conference on Seismic Discrimination*, **2**, 147-159, NTIS, Springfield, VA.

Der, Z. A., A. C. Lees, R. H. Shumway, T. W. McElfresh, and M. E. Marshall (1986). Multichannel deconvolution of P waves at seismic arrays and three-component stations, *Report TGAL-86-06*, Teledyne Geotech, Alexandria, VA.

Der, Z. A., T. W. McElfresh, R. A. Wagner, and J. Burnetti (1985). Errata to "Spectral characteristics of P waves from nuclear explosions and yield estimation", *Bull. Seism. Soc. Am.*, **75**, 1222.

Douglas, A. (1966). A special purpose least squares programme, *AWRE Report No. O-54/66*, HMSO, London, UK.

Douglas, A., J. A. Hudson, and B. J. Barley (1981). Complexity of short-period P seismograms: what does scattering contribute? *AWRE Report No. O-3/81*, HMSO, London, UK.

Douglas, A. and P. D. Marshall (1983). Comments on "Teleseismic short-period amplitudes: source and receiver variations" by R. Butler and L. Ruff, *Bull. Seism. Soc. Am.*, **73**, 667-671.

Douglas, A., P. D. Marshall, and J. B. Young (1987). The P waves from the Amchitka Island explosions, *Geophys. J. R. astr. Soc.*, **90**, 101-117.

Douglas, A., P. D. Marshall, P. G. Gibbs, J. B. Young, and C. Blamey (1973). P signal complexity re-examined, *Geophys. J. R. astr. Soc.*, **33**, 195-221.

Ericsson, U. (1971). A linear model for the yield dependent magnitudes measured by a seismograph network, *Report C4455-26*, Research Institute of National Defense,

Stockholm, Sweden.

Evernden, J. F. and D. M. Clark (1970). Study of teleseismic P. II. Amplitude data, *Phys. Earth Planet. Interiors*, **4**, 24-31.

Evernden, J. F. and G. E. Marsh (1987). Yields of U.S. and Soviet nuclear tests, *Physics Today*, **8-1**, 37-44.

Gordan, M. R. (1988). *New York Times*, October 30, 137 P.A15.

Gutenberg, B. and C. F. Richter (1956). Magnitude and energy of earthquakes, *Annali Geofis*, **9**, 1-15.

Israelson, H. (1991). RMS magnitude and path corrections for USSR explosions *(abstract)*, *EOS, Trans. A.G.U.*, **72-44**, 338.

Jih, R.-S. and K. L. McLaughlin (1988). Investigation of explosion generated SV L_g waves in 2-D heterogeneous crustal models by finite-difference method, *Report AFGL-TR-88-0025 (=TGAL-88-01)*, Geophysics Laboratory, Hanscom Air Force Base, MA. **(ADA213586)**

Jih, R.-S., K. L. McLaughlin and Z. A. Der (1988). Free boundary conditions of arbitrary polygonal topography in a 2-D explicit elastic finite difference scheme, *Geophysics*, **53**, 1045-1055.

Jih, R.-S. and R. A. Wagner (1991a). Azimuthal variation of m_b residuals of E. Kazakh explosions and assessment of the path effects *(abstract)*, *EOS, Trans. Am. Geophys. Union*, **72-17**, 193.

Jih, R.-S. and R. A. Wagner (1991b). Recent methodological developments in magnitude determination and yield estimation with applications to Semipalatinsk explosions, *Report PL-TR-91-2212(I) (=TGAL-91-05)*, Phillips Laboratory, Hanscom Air Force Base, MA. ADA244503

Jih, R.-S. and R. A. Wagner (1992). Path-corrected body-wave magnitudes and yield estimates of Semipalatinsk explosions, *Report TGAL-92-05*, Teledyne Geotech Alexandria Laboratory, Alexandria, VA

Jih, R.-S., R. A. Wagner and R. H. Shumway (1991). Magnitude-yield regression with uncertain data: a Monte-Carlo approach with applications to Semipalatinsk explosions *(abstract)*, *EOS, Trans. Am. Geophys. Union*, **72-44**, 338.

Jih, R.-S. and R. H. Shumway (1989). Iterative network magnitude estimation and uncertainty assessment with noisy and clipped data, *Bull. Seism. Soc. Am.*, **79**, 1122-1141.

Jih, R.-S., R. H. Shumway, D. W. Rivers, R. A. Wagner, and T. W. McElfresh (1990). Magnitude-yield relationship at various nuclear test sites: a maximum-likelihood approach using heavily censored yields, *Report GL-TR-90-0107 (=TGAL-90-03)*, Geophysics Laboratory, Hanscom Air Force Base, MA. **(ADA223490)**

Lay, T. (1991). Yield estimation, free-surface interactions, and tectonic release at Novaya

Zemlya, in *Proceedings of the 13th DARPA/PL Seismic Research Symposium, 8-10 October 1991, Keystone, CO (Eds J. Lewkowicz and J. McPhetres) Report PL-TR-91-2208,* Phillips Laboratory, Hanscom Air Force Base, MA. **(ADA241325)**

Lay, T. and J. L. Welc (1987). Analysis of near-source contribution to early *P*–wave coda for underground explosions. I. waveform complexity, *Bull. Seism. Soc. Am.,* **77-3,** 1017-1040.

Leith, W. and J. Unger (1989). Three-dimensional geological modeling of the Shagan River nuclear test site, paper presented at *DARPA/AFTAC Annual Seismic Research Review,* Patrick AFB, FL.

Leith, W., J. R. Matzko, J. Unger, and D. W. Simpson (1990). Geology and image analysis of the Soviet nuclear test site at Matochkin Shar, Novaya Zemlya, U.S.S.R., in *Proceedings of the 12th DARPA/GL Seismic Research Symposium, 18-20 Sept 1990, Key West, FL,* (Eds J. Lewkowicz and J. McPhetres), *Report GL-TR-90-0212,* Geophysics Laboratory, Hanscom Air Force Base, MA. **(ADA226635)**

Lilwall, R. C. and J. M. Neary (1985). Redetermination of earthquake body-wave magnitudes using ISC Bulletin data, *AWRE Report No. O-21/85, HMSO, London, UK.*

Lilwall, R. C. and P. D. Marshall (1986). Body-wave magnitudes and locations of Soviet underground explosions at the Novaya Zemlya Test Site, *AWE Report O-17/86,* HMSO, London, UK.

Lilwall, R. C., P. D. Marshall, and D. W. Rivers (1988). Body wave magnitudes of some underground nuclear explosions at the Nevada (USA) and Shagan River (USSR) Test Sites, *AWE Report O-15/88,* HMSO, London, UK.

Marshall, P. D. (1972). Some seismic results from a worldwide sample of large underground explosions, *AWRE Report O-49/72,* HMSO, London, UK.

Marshall, P. D., D. L. Springer, and H. C. Rodean (1979). Magnitude corrections for attenuation in the upper mantle, *Geophys. J. R. astr. Soc.,* **57,** 609-638.

Marshall, P. D., T. C. Bache, and R. C. Lilwall, R. C. (1984). Body wave magnitudes and locations of Soviet underground explosions at the Semipalatinsk Test Site, *AWE Report O-16/84,* HMSO, London, UK.

McLaughlin, K. L., and R.-S. Jih (1986). Finite-difference simulations of Rayleigh wave scattering by 2-D rough topography, *Report AFGL-TR-86-0269 (=TGAL-86-09),* Geophysics Laboratory, Hanscom Air Force Base, MA. **(ADA179190)**

McLaughlin, K. L., and R.-S. Jih (1987). Finite-difference simulations of Rayleigh wave scattering by 2-D shallow heterogeneity, *Report AFGL-TR-87-0322 (=TGAL-87-02),* Geophysics Laboratory, Hanscom Air Force Base, MA. **(ADA194961)**

McLaughlin, K. L., and R.-S. Jih (1988). Scattering from near-source topography: teleseismic observations and numerical simulations, *Bull. Seism. Soc. Am.,* **78-4,** 1399-1414.

Miller, S. A. and A. L. Florence (1991). Laboratory particle velocity experiments on Indiana limestone and Sirra white granite, *Report PL-TR-91-2277*, Phillips Laboratory, Hanscom Air Force Base, MA. ADA248045

Murphy, J. R., B. W. Barker, and A. O'Donnell (1989). Network-averaged teleseismic *P*-wave spectra for underground explosions. Part I - Definitions and Examples, *Bull. Seism. Soc. Am.*, **79-1**, 141-155.

North, R. G. (1977). Station magnitude bias --- its determination, causes, and effects, *Lincoln Laboratory, Technical Report 1977-24*, Massachusetts Institute of Technology, Lexington, MA.

Nuttli, O. W. (1986a). Yield estimates of Nevada Test Site explosions obtained from seismic L_g waves, *J. Geophys. Res.*, **91**, 2137-2151.

Nuttli, O. W. (1986b). L_g magnitudes of selected East Kazakhstan underground explosions, *Bull. Seism. Soc. Am.*, **76**, 1241-1251.

Nuttli, O. W. (1987). L_g magnitudes of Degelen, East Kazakhstan, underground explosions, *Bull. Seism. Soc. Am.*, **77**, 679-681.

Nuttli, O. W. (1988). Lg magnitudes and yield estimates for underground Novaya Zemlya nuclear explosions, *Bull. Seism. Soc. Am.*, **78**, 873-884.

Patton, H. J. (1988). Application of Nuttli's method to estimate yield of Nevada Test Site explosions recorded on Lawrence Livermore National Laboratory's digital seismic system, *Bull. Seism. Soc. Am.*, **78**, 1759-1772.

Perry, R. K., H. S. Fleming, I. R. Weber, Y. Kristoffersen, J. K. Hall, A. Grantz, G. L. Johnson, N. Z. Cherkis, and B. Larsen (1986). Bathymetry of the Arctic Ocean, *MC-56*, Acoustic Media Characterization Branch, Acoustics Division, Naval Research Laboratory, Washington, DC.

Ringdal, F. (1976). Maximum likelihood estimation of seismic magnitude, *Bull. Seism. Soc. Am.*, **66**, 789-802.

Ringdal, F. (1986). Study of magnitudes, seismicity, and earthquake detectability using a global network, *Bull. Seism. Soc. Am.*, **76**, 1641-1659.

Ringdal, F. and J. Fyen (1991). RMS Lg analysis of Novaya Zemlya explosion recordings, Semiannual Technical Summary, 1 Oct 1990 - 31 Mar 1991, *NORSAR Scientific Report No.2-90/91*, NTNF/NORSAR, Kjeller, Norway (May 1991).

Ringdal, F. and P. D. Marshall (1989). Yield determination of Soviet underground nuclear explosions at the Shagan River Test Site, Semiannual Technical Summary, 1 Oct 1988 - 31 Mar 1989 (L. B. Loughran ed.), *NORSAR Scientific Report No.2-88/89*, NTNF/NORSAR, Kjeller, Norway.

Samuel, P. (1985). *Defense Week*, 5 August, page 1.

Sleep, N. H. (1973). Teleseismic P–wave transmission through slabs, *Bull. Seism. Soc. Am.*, **63-4,** 1349-1373.

Solomon, S. and M. N. Toksoz (1970). Lateral variation of attenuation of P and S waves beneath the United States, *Bull. Seism. Soc. Am.*, **60,** 819-838.

Stewart, R. C. and P. D. Marshall (1988). Seismic P waves from Novaya Zemlya explosions: seeing double! *Geophys. J.,* **92,** 335-338.

Sykes, L. R. (1985). letter to D. B. Fascell, chairman of House Foreign Affairs Committee, 30 August.

Sykes, L. R. and I. Cifuentes (1984). Yields of Soviet underground nuclear explosions from seismic surface waves: compliance with the threshold test ban treaty, *Proc. Natl. Acad. Sci. USA,* **81,** 1922-1925.

Sykes, L. R. and G. C. Wiggins (1986). Yields of Soviet underground nuclear explosions at Novaya Zemlya, 1964-1976, from seismic body and surface waves, *Proc. Natl. Acad. Sci. USA,* **83,** 201-205.

Sykes, L. R. and D. M. Davis (1987). The yields of Soviet strategic weapons, *Scientific American,* **256-1,** 29-37.

Sykes, L. R. and S. Ruggi (1989). Soviet nuclear testing, in *Nuclear Weapon Databook* (Volume IV, Chapter 10), Natural Resources Defense Concil, Washington D. C.

Veith, K. F. and G. E. Clawson (1972). Magnitude from short-period P–wave data, *Bull. Seism. Soc. Am.*, **62,** 435-452.

Vergino, E. S. (1989). Soviet test yields, *EOS, Trans. A.G.U.*, Nov 28, 1989.

von Seggern, D. H. (1973). Joint magnitude determination and analysis of variance for explosion magnitude estimates, *Bull. Seism. Soc. Am.*, **63,** 827-845.

von Seggern, D. H. and D. W. Rivers (1978). Comments on the use of truncated distribution theory for improved magnitude estimation, *Bull. Seism. Soc. Am.*, **68,** 1543-1546.

Zeng, Y. H., J. Faulkner, T. L. Teng, and K. Aki (1986). Focusing and defocusing of Rayleigh waves from USSR across Arctic region, *EOS, Trans. A.G.U.*, **68-44,** 1377.

APPENDIX: YIELD ESTIMATES OF SEMIPALATINSK EXPLOSIONS

The accuracy of our absolute yield estimates of Novaya Zemlya explosions presented in this study rely on that of Semipalatinsk explosions as well as the validity of the comparable-coupling assumption. It is fortuitous to have the source information by Bocharov *et al.* (1989) (and Vergino, 1989) to calibrate the Semipalatinsk test site. The small scatter around the following calibration curves based on the regression of our path-corrected m_b on the published yields illustrates how well the fit can be at the Central Asian test site. Detailed discussion can be found in Jih and Wagner (1992).

$$m_b(P_a) = 0.802(\pm 0.020) \log(W) + 3.834(\pm 0.032)$$

$$m_b(P_b) = 0.800(\pm 0.020) \log(W) + 4.130(\pm 0.031)$$

$$m_b(P_{max}) = 0.768(\pm 0.019) \log(W) + 4.399(\pm 0.030)$$

We have utilized these calibration curves to estimate the yield of all Semipalatinsk explosions in our data set, and the result is summarized in the following Tables. For the cratering events (such as 650115B) the yield estimate based on the first motion (*i.e.*, P_a) should be used, since no depth correction (*e.g.*, Marshall *et al.*, 1979) has been applied to $m_b(P_b)$ or $m_b(P_{max})$ in our study. Note the excellent match between the announced yield (100-150 KT) of 650115B and the predicted value (111 KT). Another example is the Soviet Joint Verification Experiment [JVE] of 880914B, which is said to have an on-site hydrodynamic yield measurement of 115 KT (Gordan, 1988). Both examples illustrate, again, that P_a from hard-rock test sites in stable region could be a very favorable phase for the source size determination. The $m_b(P_{max})$ of 25 Balapan events for which the $m_b(P_b)$ and $m_b(P_a)$ are missing are based on m_b values published by Lilwall *et al.* (1988). A correction to convert the B(Δ) (*cf.* Equation [1]) of Gutenberg and Richter (1956) to that of Veith and Clawson (1972) is applied to every station m_b before these recordings are incorporated into our data set.

Magnitudes of Semipalatinsk Explosions							
Event		# of Signals	Magnitudes (Jih and Wagner,1992)				Yield
Date	Site	Ns Nn Nc	S.E.M.	P_a	P_b	P_{max}	
650115B	BTZ	45 1 2	0.028	5.473	5.709	5.865	100-150
651121D	Deg	48 15 1	0.024	4.962	5.240	5.452	29
660213D	Deg	51 4 10	0.024	5.717	5.965	6.152	125
660320D	Deg	49 9 8	0.024	5.416	5.697	5.916	100
660507D	Deg	9 26 1	0.033	4.089	4.237	4.529	4
661019D	Deg	51 10 5	0.024	5.164	5.423	5.596	20-150
661218M	Mzk	55 8 1	0.024	5.395	5.632	5.852	20-150
670226D	Deg	48 9 6	0.025	5.438	5.688	5.914	20-150
670916M	Mzk	36 29 2	0.024	4.657	4.937	5.182	<20
670922M	Mzk	35 31 1	0.024	4.516	4.840	5.118	10
671122M	Mzk	7 63 0	0.023	____	3.975	4.353	<20
680619B	BNE	28 3 2	0.034	4.666	5.002	5.256	<20
680929D	Deg	50 7 6	0.025	5.222	5.511	5.710	60
690531M	Mzk	30 30 0	0.025	4.468	4.885	5.115	<20
690723D	Deg	38 20 1	0.025	4.711	5.022	5.248	16
690911D	Deg	19 38 0	0.026	4.141	4.381	4.709	<20
691130B	BTZ	49 0 0	0.028	5.362	5.733	5.915	125
691228M	Mzk	45 9 3	0.026	5.264	5.551	5.753	46
700721M	Mzk	38 20 1	0.025	4.689	5.033	5.281	<20
701104M	Mzk	38 22 1	0.025	4.934	5.137	5.349	<20
710322D	Deg	43 14 3	0.025	5.117	5.408	5.587	20-150
710425D	Deg	37 5 0	0.030	5.434	5.696	5.891	90
710606M	Mzk	38 12 2	0.027	4.879	5.218	5.425	16

Magnitudes of Semipalatinsk Explosions							
Event		# of Signals	Magnitudes (Jih and Wagner,1992)				Yield
Date	Site	Ns Nn Nc	S.E.M.	P_a	P_b	P_{max}	
710619M	Mzk	41 13 0	0.027	4.863	5.162	5.392	<20
710630B	BTZ	31 19 1	0.027	4.448	4.766	5.036	<20
711009M	Mzk	27 12 3	0.030	4.791	5.026	5.226	12
711021M	Mzk	32 9 0	0.031	4.875	5.208	5.442	23
711230D	Deg	16 3 0	0.045	5.080	5.425	5.610	20-150
720210B	BNE	34 8 2	0.029	4.811	5.073	5.306	16
720328D	Deg	28 17 0	0.029	4.481	4.826	5.051	6
720816D	Deg	23 23 1	0.029	4.447	4.735	4.991	8
720826M	Mzk	29 15 2	0.029	4.688	5.033	5.258	<20
720902M	Mzk	15 29 0	0.029	4.148	4.405	4.682	2
721102B	BSW	42 1 15	0.026	5.619	5.935	6.158	165
721210D	Deg	30 7 5	0.030	5.075	5.402	5.624	20-150
721210B	BNE	44 2 11	0.026	____	5.801	5.998	140
730723B	BTZ	52 1 1	0.027	5.743	5.985	6.171	__
731214B	BNE	49 8 6	0.025	5.248	5.549	5.760	__
750427B	BNE	18 1 1	0.044	4.904	5.238	5.521	__
760704B	BTZ	38 0 5	0.030	5.199	5.545	5.812	__
761123B	BNE	22 0 0	0.042	____	____	5.680	__
761207B	BSW	17 2 1	0.044	4.928	5.351	5.581	__
770329D	Deg	25 14 0	0.031	4.401	4.785	5.073	__
770730D	Deg	21 16 0	0.032	4.296	4.692	4.943	__
780326D	Deg	25 6 0	0.035	4.995	5.301	5.530	__
780422D	Deg	21 9 0	0.036	4.562	4.821	5.071	__

Magnitudes of Semipalatinsk Explosions							
Event		# of Signals	Magnitudes (Jih and Wagner,1992)				Yield
Date	Site	Ns Nn Nc	S.E.M.	P_a	P_b	P_{max}	
780611B	BSW	17 0 1	0.046	5.246	5.513	5.811	___
780705B	BSW	38 7 7	0.027	5.215	5.489	5.738	___
780728D	Deg	36 9 6	0.027	5.068	5.365	5.577	___
780829B	BNE	16 0 0	0.049	___	___	5.926	___
780915B	BTZ	36 1 6	0.030	5.414	5.655	5.828	___
781104B	BNE	40 9 6	0.026	5.109	5.349	5.566	___
781129B	BSW	28 0 0	0.037	___	___	5.886	___
790623B	BTZ	40 2 3	0.029	5.639	5.878	6.084	___
790707B	BNE	30 0 0	0.036	___	___	5.812	___
790804B	BSW	40 4 20	0.024	5.609	5.894	6.114	HE*
790818B	BNE	28 0 0	0.037	___	___	6.095	___
791028B	BNE	44 5 13	0.025	5.463	5.700	5.932	HE
791202B	BSW	15 0 0	0.050	___	___	5.900	___
791223B	BSW	40 3 17	0.025	5.599	5.890	6.139	HE
800522D	Deg	36 22 1	0.025	4.721	4.980	5.188	___
800629B	BSW	46 5 6	0.026	5.202	5.455	5.664	___
800914B	BTZ	34 5 6	0.029	5.493	5.824	6.087	___
801012B	BNE	23 0 0	0.041	___	___	5.856	___
801214B	BTZ	28 0 0	0.037	___	___	5.919	___
801227B	BNE	24 0 0	0.040	___	___	5.899	___
810422B	BSW	25 0 0	0.039	___	___	5.922	___
810913B	BTZ	17 0 0	0.047	___	___	6.077	___
811018B	BSW	41 3 7	0.027	5.492	5.778	5.989	HE

*: a historical event discussed at U.S.-U.S.S.R. negotiation.

Magnitudes of Semipalatinsk Explosions							
Event		# of Signals	Magnitudes (Jih and Wagner,1992)				Yield
Date	Site	Ns Nn Nc	S.E.M.	P_a	P_b	P_{max}	
811129B	BSW	37 11 5	0.027	5.044	5.313	5.527	——
811227B	BSW	23 0 0	0.041	——	——	6.196	——
820425B	BTZ	14 0 0	0.052	——	——	5.970	——
820704B	BTZ	21 0 0	0.043	——	——	6.054	——
820831B	BSW	27 17 1	0.029	4.559	4.865	5.097	——
821205B	BSW	26 0 0	0.038	——	——	6.108	——
821226B	BNE	38 10 1	0.028	5.171	5.378	5.606	——
830612B	BTZ	16 0 0	0.049	——	——	5.940	——
831006B	BSW	25 0 0	0.039	——	——	5.939	——
831026B	BTZ	18 0 0	0.046	——	——	5.989	——
831120B	BNE	17 8 3	0.037	4.933	5.130	5.339	——
840425B	BTZ	21 0 0	0.043	——	——	5.895	——
840526B	BNE	31 0 3	0.034	5.547	5.848	6.005	HE
840714B	BTZ	22 0 0	0.042	——	——	6.057	——
841027B	BSW	19 0 0	0.045	——	——	6.233	——
841202B	BNE	22 0 0	0.042	——	——	5.709	——
841216B	BTZ	15 0 0	0.050	——	——	6.038	——
841228B	BSW	19 0 0	0.045	——	——	5.924	——
850210B	BSW	18 1 4	0.041	5.309	5.585	5.834	——
850615B	BSW	15 0 0	0.050	——	——	6.060	——
850630B	BSW	37 3 6	0.029	5.406	5.679	5.898	——
870620B	BSW	24 3 13	0.031	5.520	5.766	5.999	——
880914B	BSW	25 0 1	0.038	5.480	5.777	6.021	JVE*

*: Joint Verification Experiment.

Yield Estimates of Semipalatinsk Explosions							
Event		Epicenter		Yield (Jih and Wagner, 1992)			Yield
Date	Site	Lon	Lat	P_a	P_b	P_{max}	Announced
650115B	BTZ	79.009	49.935	111	94	81	100-150
651121D	Deg	78.064	49.819	25	24	24	29
660213D	Deg	78.121	49.809	223	197	192	125
660320D	Deg	78.024	49.762	94	91	94	100
660507D	Deg	78.105	49.743	2	1	1	4
661019D	Deg	78.021	49.747	46	41	36	20-150
661218M	Mzk	77.747	49.925	88	75	78	20-150
670226D	Deg	78.082	49.746	100	89	94	20-150
670916M	Mzk	77.728	49.937	11	10	10	<20
670922M	Mzk	77.691	49.960	7	8	9	10
671122M	Mzk	77.687	49.942	—	1	1	<20
680619B	BNE	78.986	49.980	11	12	13	<20
680929D	Deg	78.122	49.812	54	53	51	60
690531M	Mzk	77.694	49.950	6	9	9	<20
690723D	Deg	78.130	49.816	12	13	13	16
690911D	Deg	77.997	49.776	2	2	3	<20
691130B	BTZ	78.956	49.924	80	101	94	125
691228M	Mzk	77.714	49.937	61	60	58	46
700721M	Mzk	77.673	49.952	12	13	14	<20
701104M	Mzk	77.762	49.989	24	18	17	<20
710322D	Deg	78.109	49.798	40	40	35	20-150
710425D	Deg	78.034	49.769	99	91	88	90
710606M	Mzk	77.660	49.975	20	23	22	16

Yield Estimates of Semipalatinsk Explosions							
Event		Epicenter		Yield (Jih and Wagner, 1992)			Yield
Date	Site	Lon	Lat	P_a	P_b	P_{max}	Announced
710619M	Mzk	77.641	49.969	19	19	20	<20
710630B	BTZ	78.980	49.946	6	6	7	<20
711009M	Mzk	77.641	49.978	16	13	12	12
711021M	Mzk	77.597	49.974	20	22	23	23
711230D	Deg	78.037	49.760	36	42	38	20-150
720210B	BNE	78.878	50.024	17	15	15	16
720328D	Deg	78.076	49.733	6	7	7	6
720816D	Deg	78.059	49.765	6	6	6	8
720826M	Mzk	77.717	49.982	12	13	13	<20
720902M	Mzk	77.641	49.959	2	2	2	2
721102B	BSW	78.817	49.927	168	180	195	165
721210D	Deg	78.058	49.819	35	39	39	20-150
721210B	BNE	78.996	50.027	—	123	121	140
730723B	BTZ	78.850	49.980	240	208	203	—
731214B	BNE	79.010	50.040	58	59	59	—
750427B	BNE	78.980	49.990	22	24	29	—
760704B	BTZ	78.950	49.910	50	59	69	—
761123B	BNE	79.000	49.990	—	—	47	—
761207B	BSW	78.900	49.880	23	34	35	—
770329D	Deg	78.140	49.790	5	7	8	—
770730D	Deg	78.160	49.770	4	5	5	—
780326D	Deg	78.070	49.730	28	29	30	—
780422D	Deg	78.170	49.720	8	7	7	—

Yield Estimates of Semipalatinsk Explosions							
Event		Epicenter		Yield (Jih and Wagner, 1992)			Yield
Date	Site	Lon	Lat	P_a	P_b	P_{max}	Announced
780611B	BSW	78.838	49.879	58	54	69	—
780705B	BSW	78.871	49.887	53	50	55	—
780728D	Deg	78.140	49.756	35	35	34	—
780829B	BNE	78.990	50.000	—	—	97	—
780915B	BTZ	78.940	49.910	93	81	73	—
781104B	BNE	78.943	50.034	39	33	33	—
781129B	BSW	78.760	49.950	—	—	86	—
790623B	BTZ	78.910	49.910	178	153	156	—
790707B	BNE	79.060	50.050	—	—	69	—
790804B	BSW	78.904	49.894	163	160	171	HE
790818B	BNE	79.010	49.970	—	—	162	—
791028B	BNE	78.997	49.973	107	92	99	HE
791202B	BSW	78.840	49.890	—	—	90	—
791223B	BSW	78.755	49.916	159	158	184	HE
800522D	Deg	78.082	49.784	13	12	11	—
800629B	BSW	78.815	49.939	51	45	44	—
800914B	BTZ	78.880	49.970	117	131	158	—
801012B	BNE	79.080	49.950	—	—	79	—
801214B	BTZ	79.000	49.930	—	—	95	—
801227B	BNE	79.040	50.040	—	—	90	—
810422B	BSW	78.900	49.900	—	—	96	—
810913B	BTZ	78.980	49.890	—	—	153	—
811018B	BSW	78.859	49.923	117	115	118	HE

Yield Estimates of Semipalatinsk Explosions							
Event		Epicenter		Yield (Jih and Wagner, 1992)			Yield
Date	Site	Lon	Lat	P_a	P_b	P_{max}	Announced
811129B	BSW	78.860	49.887	32	30	29	—
811227B	BSW	78.870	49.900	—	—	219	—
820425B	BTZ	78.930	49.880	—	—	111	—
820704B	BTZ	78.850	49.990	—	—	143	—
820831B	BSW	78.761	49.924	8	8	8	—
821205B	BSW	78.840	49.910	—	—	168	—
821226B	BNE	78.988	50.071	46	36	37	—
830612B	BTZ	78.980	49.910	—	—	102	—
831006B	BSW	78.840	49.930	—	—	101	—
831026B	BTZ	78.910	49.920	—	—	118	—
831120B	BNE	78.999	50.047	23	18	17	—
840425B	BTZ	78.940	49.950	—	—	89	—
840526B	BNE	79.006	49.969	137	140	123	HE
840714B	BTZ	78.960	49.890	—	—	144	—
841027B	BSW	78.830	49.950	—	—	244	—
841202B	BNE	79.070	49.990	—	—	51	—
841216B	BTZ	78.860	49.960	—	—	136	—
841228B	BSW	78.750	49.860	—	—	97	—
850210B	BSW	78.781	49.888	69	66	74	—
850615B	BSW	78.880	49.890	—	—	145	—
850630B	BSW	78.658	49.848	91	86	89	—
870620B	BSW	78.740	49.927	127	111	121	—
880914B	BSW	78.808	49.833	113	114	129	JVE

Prof. Thomas Ahrens
Seismological Lab, 252-21
Division of Geological & Planetary Sciences
California Institute of Technology
Pasadena, CA 91125

Prof. Keiiti Aki
Center for Earth Sciences
University of Southern California
University Park
Los Angeles, CA 90089-0741

Prof. Shelton Alexander
Geosciences Department
403 Deike Building
The Pennsylvania State University
University Park, PA 16802

Dr. Ralph Alewine, III
DARPA/NMRO
3701 North Fairfax Drive
Arlington, VA 22203-1714

Prof. Charles B. Archambeau
CIRES
University of Colorado
Boulder, CO 80309

Dr. Thomas C. Bache, Jr.
Science Applications Int'l Corp.
10260 Campus Point Drive
San Diego, CA 92121 (2 copies)

Prof. Muawia Barazangi
Institute for the Study of the Continent
Cornell University
Ithaca, NY 14853

Dr. Jeff Barker
Department of Geological Sciences
State University of New York
 at Binghamton
Vestal, NY 13901

Dr. Douglas R. Baumgardt
ENSCO, Inc
5400 Port Royal Road
Springfield, VA 22151-2388

Dr. Susan Beck
Department of Geosciences
Building #77
University of Arizona
Tuscon, AZ 85721

Dr. T.J. Bennett
S-CUBED
A Division of Maxwell Laboratories
11800 Sunrise Valley Drive, Suite 1212
Reston, VA 22091

Dr. Robert Blandford
AFTAC/TT, Center for Seismic Studies
1300 North 17th Street
Suite 1450
Arlington, VA 22209-2308

Dr. G.A. Bollinger
Department of Geological Sciences
Virginia Polytechnical Institute
21044 Derring Hall
Blacksburg, VA 24061

Dr. Stephen Bratt
Center for Seismic Studies
1300 North 17th Street
Suite 1450
Arlington, VA 22209-2308

Dr. Lawrence Burdick
Woodward-Clyde Consultants
566 El Dorado Street
Pasadena, CA 91109-3245

Dr. Robert Burridge
Schlumberger-Doll Research Center
Old Quarry Road
Ridgefield, CT 06877

Dr. Jerry Carter
Center for Seismic Studies
1300 North 17th Street
Suite 1450
Arlington, VA 22209-2308

Dr. Eric Chael
Division 9241
Sandia Laboratory
Albuquerque, NM 87185

Prof. Vernon F. Cormier
Department of Geology & Geophysics
U-45, Room 207
University of Connecticut
Storrs, CT 06268

Prof. Steven Day
Department of Geological Sciences
San Diego State University
San Diego, CA 92182

Marvin Denny
U.S. Department of Energy
Office of Arms Control
Washington, DC 20585

Dr. Zoltan Der
ENSCO, Inc.
5400 Port Royal Road
Springfield, VA 22151-2388

Prof. Adam Dziewonski
Hoffman Laboratory, Harvard University
Dept. of Earth Atmos. & Planetary Sciences
20 Oxford Street
Cambridge, MA 02138

Prof. John Ebel
Department of Geology & Geophysics
Boston College
Chestnut Hill, MA 02167

Eric Fielding
SNEE Hall
INSTOC
Cornell University
Ithaca, NY 14853

Dr. Mark D. Fisk
Mission Research Corporation
735 State Street
P.O. Drawer 719
Santa Barbara, CA 93102

Prof Stanley Flatte
Applied Sciences Building
University of California, Santa Cruz
Santa Cruz, CA 95064

Dr. John Foley
NER-Geo Sciences
1100 Crown Colony Drive
Quincy, MA 02169

Prof. Donald Forsyth
Department of Geological Sciences
Brown University
Providence, RI 02912

Dr. Art Frankel
U.S. Geological Survey
922 National Center
Reston, VA 22092

Dr. Cliff Frolich
Institute of Geophysics
8701 North Mopac
Austin, TX 78759

Dr. Holly Given
IGPP, A-025
Scripps Institute of Oceanography
University of California, San Diego
La Jolla, CA 92093

Dr. Jeffrey W. Given
SAIC
10260 Campus Point Drive
San Diego, CA 92121

Dr. Dale Glover
Defense Intelligence Agency
ATTN: ODT-1B
Washington, DC 20301

Dr. Indra Gupta
Teledyne Geotech
314 Montgomery Street
Alexanderia, VA 22314

Dan N. Hagedon
Pacific Northwest Laboratories
Battelle Boulevard
Richland, WA 99352

Dr. James Hannon
Lawrence Livermore National Laboratory
P.O. Box 808
L-205
Livermore, CA 94550

Dr. Roger Hansen
HQ AFTAC/TTR
Patrick AFB, FL 32925-6001

Prof. David G. Harkrider
Seismological Laboratory
Division of Geological & Planetary Sciences
California Institute of Technology
Pasadena, CA 91125

Prof. Danny Harvey
CIRES
University of Colorado
Boulder, CO 80309

Prof. Donald V. Helmberger
Seismological Laboratory
Division of Geological & Planetary Sciences
California Institute of Technology
Pasadena, CA 91125

Prof. Charles A. Langston
Geosciences Department
403 Deike Building
The Pennsylvania State University
University Park, PA 16802

Prof. Eugene Herrin
Institute for the Study of Earth and Man
Geophysical Laboratory
Southern Methodist University
Dallas, TX 75275

Jim Lawson, Chief Geophysicist
Oklahoma Geological Survey
Oklahoma Geophysical Observatory
P.O. Box 8
Leonard, OK 74043-0008

Prof. Robert B. Herrmann
Department of Earth & Atmospheric Sciences
St. Louis University
St. Louis, MO 63156

Prof. Thorne Lay
Institute of Tectonics
Earth Science Board
University of California, Santa Cruz
Santa Cruz, CA 95064

Prof. Lane R. Johnson
Seismographic Station
University of California
Berkeley, CA 94720

Dr. William Leith
U.S. Geological Survey
Mail Stop 928
Reston, VA 22092

Prof. Thomas H. Jordan
Department of Earth, Atmospheric &
  Planetary Sciences
Massachusetts Institute of Technology
Cambridge, MA 02139

Mr. James F. Lewkowicz
Phillips Laboratory/GPEH
Hanscom AFB, MA 01731-5000(2 copies)

Prof. Alan Kafka
Department of Geology & Geophysics
Boston College
Chestnut Hill, MA 02167

Mr. Alfred Lieberman
ACDA/VI-OA State Department Building
Room 5726
320-21st Street, NW
Washington, DC 20451

Robert C. Kemerait
ENSCO, Inc.
445 Pineda Court
Melbourne, FL 32940

Prof. L. Timothy Long
School of Geophysical Sciences
Georgia Institute of Technology
Atlanta, GA 30332

Dr. Max Koontz
U.S. Dept. of Energy/DP 5
Forrestal Building
1000 Independence Avenue
Washington, DC 20585

Dr. Randolph Martin, III
New England Research, Inc.
76 Olcott Drive
White River Junction, VT 05001

Dr. Richard LaCoss
MIT Lincoln Laboratory, M-200B
P.O. Box 73
Lexington, MA 02173-0073

Dr. Robert Masse
Denver Federal Building
Box 25046, Mail Stop 967
Denver, CO 80225

Dr. Fred K. Lamb
University of Illinois at Urbana-Champaign
Department of Physics
1110 West Green Street
Urbana, IL 61801

Dr. Gary McCartor
Department of Physics
Southern Methodist University
Dallas, TX 75275

Prof. Thomas V. McEvilly
Seismographic Station
University of California
Berkeley, CA 94720

Prof. John A. Orcutt
IGPP, A-025
Scripps Institute of Oceanography
University of California, San Diego
La Jolla, CA 92093

Dr. Art McGarr
U.S. Geological Survey
Mail Stop 977
U.S. Geological Survey
Menlo Park, CA 94025

Prof. Jeffrey Park
Kline Geology Laboratory
P.O. Box 6666
New Haven, CT 06511-8130

Dr. Keith L. McLaughlin
S-CUBED
A Division of Maxwell Laboratory
P.O. Box 1620
La Jolla, CA 92038-1620

Dr. Howard Patton
Lawrence Livermore National Laboratory
L-025
P.O. Box 808
Livermore, CA 94550

Stephen Miller & Dr. Alexander Florence
SRI International
333 Ravenswood Avenue
Box AF 116
Menlo Park, CA 94025-3493

Dr. Frank Pilotte
HQ AFTAC/TT
Patrick AFB, FL 32925-6001

Prof. Bernard Minster
IGPP, A-025
Scripps Institute of Oceanography
University of California, San Diego
La Jolla, CA 92093

Dr. Jay J. Pulli
Radix Systems, Inc.
2 Taft Court, Suite 203
Rockville, MD 20850

Prof. Brian J. Mitchell
Department of Earth & Atmospheric Sciences
St. Louis University
St. Louis, MO 63156

Dr. Robert Reinke
ATTN: FCTVTD
Field Command
Defense Nuclear Agency
Kirtland AFB, NM 87115

Mr. Jack Murphy
S-CUBED
A Division of Maxwell Laboratory
11800 Sunrise Valley Drive, Suite 1212
Reston, VA 22091 (2 Copies)

Prof. Paul G. Richards
Lamont-Doherty Geological Observatory
 of Columbia University
Palisades, NY 10964

Dr. Keith K. Nakanishi
Lawrence Livermore National Laboratory
L-025
P.O. Box 808
Livermore, CA 94550

Mr. Wilmer Rivers
Teledyne Geotech
314 Montgomery Street
Alexandria, VA 22314

Dr. Carl Newton
Los Alamos National Laboratory
P.O. Box 1663
Mail Stop C335, Group ESS-3
Los Alamos, NM 87545

Dr. George Rothe
HQ AFTAC/TTR
Patrick AFB, FL 32925-6001

Dr. Bao Nguyen
HQ AFTAC/TTR
Patrick AFB, FL 32925-6001

Dr. Alan S. Ryall, Jr.
DARPA/NMRO
3701 North Fairfax Drive
Arlington, VA 22209-1714

Dr. Richard Sailor
TASC, Inc.
55 Walkers Brook Drive
Reading, MA 01867

Donald L. Springer
Lawrence Livermore National Laboratory
L-025
P.O. Box 808
Livermore, CA 94550

Prof. Charles G. Sammis
Center for Earth Sciences
University of Southern California
University Park
Los Angeles, CA 90089-0741

Dr. Jeffrey Stevens
S-CUBED
A Division of Maxwell Laboratory
P.O. Box 1620
La Jolla, CA 92038-1620

Prof. Christopher H. Scholz
Lamont-Doherty Geological Observatory
 of Columbia University
Palisades, CA 10964

Lt. Col. Jim Stobie
ATTN: AFOSR/NL
Bolling AFB
Washington, DC 20332-6448

Dr. Susan Schwartz
Institute of Tectonics
1156 High Street
Santa Cruz, CA 95064

Prof. Brian Stump
Institute for the Study of Earth & Man
Geophysical Laboratory
Southern Methodist University
Dallas, TX 75275

Secretary of the Air Force
(SAFRD)
Washington, DC 20330

Prof. Jeremiah Sullivan
University of Illinois at Urbana-Champaign
Department of Physics
1110 West Green Street
Urbana, IL 61801

Office of the Secretary of Defense
DDR&E
Washington, DC 20330

Prof. L. Sykes
Lamont-Doherty Geological Observatory
 of Columbia University
Palisades, NY 10964

Thomas J. Sereno, Jr.
Science Application Int'l Corp.
10260 Campus Point Drive
San Diego, CA 92121

Dr. David Taylor
ENSCO, Inc.
445 Pineda Court
Melbourne, FL 32940

Dr. Michael Shore
Defense Nuclear Agency/SPSS
6801 Telegraph Road
Alexandria, VA 22310

Dr. Steven R. Taylor
Los Alamos National Laboratory
P.O. Box 1663
Mail Stop C335
Los Alamos, NM 87545

Dr. Matthew Sibol
Virginia Tech
Seismological Observatory
4044 Derring Hall
Blacksburg, VA 24061-0420

Prof. Clifford Thurber
University of Wisconsin-Madison
Department of Geology & Geophysics
1215 West Dayton Street
Madison, WS 53706

Prof. David G. Simpson
IRIS, Inc.
1616 North Fort Myer Drive
Suite 1440
Arlington, VA 22209

Prof. M. Nafi Toksoz
Earth Resources Lab
Massachusetts Institute of Technology
42 Carleton Street
Cambridge, MA 02142

Dr. Larry Turnbull
CIA-OSWR/NED
Washington, DC 20505

DARPA/RMO/SECURITY OFFICE
3701 North Fairfax Drive
Arlington, VA 22203-1714

Dr. Gregory van der Vink
IRIS, Inc.
1616 North Fort Myer Drive
Suite 1440
Arlington, VA 22209

HQ DNA
ATTN: Technical Library
Washington, DC 20305

Dr. Karl Veith
EG&G
5211 Auth Road
Suite 240
Suitland, MD 20746

Defense Intelligence Agency
Directorate for Scientific & Technical Intelligence
ATTN: DTIB
Washington, DC 20340-6158

Prof. Terry C. Wallace
Department of Geosciences
Building #77
University of Arizona
Tuscon, AZ 85721

Defense Technical Information Center
Cameron Station
Alexandria, VA 22314 (2 Copies)

Dr. Thomas Weaver
Los Alamos National Laboratory
P.O. Box 1663
Mail Stop C335
Los Alamos, NM 87545

TACTEC
Battelle Memorial Institute
505 King Avenue
Columbus, OH 43201 (Final Report)

Dr. William Wortman
Mission Research Corporation
8560 Cinderbed Road
Suite 700
Newington, VA 22122

Phillips Laboratory
ATTN: XPG
Hanscom AFB, MA 01731-5000

Prof. Francis T. Wu
Department of Geological Sciences
State University of New York
 at Binghamton
Vestal, NY 13901

Phillips Laboratory
ATTN: GPE
Hanscom AFB, MA 01731-5000

AFTAC/CA
(STINFO)
Patrick AFB, FL 32925-6001

Phillips Laboratory
ATTN: TSML
Hanscom AFB, MA 01731-5000

DARPA/PM
3701 North Fairfax Drive
Arlington, VA 22203-1714

Phillips Laboratory
ATTN: SUL
Kirtland, NM 87117 (2 copies)

DARPA/RMO/RETRIEVAL
3701 North Fairfax Drive
Arlington, VA 22203-1714

Dr. Michel Bouchon
I.R.I.G.M.-B.P. 68
38402 St. Martin D'Heres
Cedex, FRANCE

Dr. Michel Campillo
Observatoire de Grenoble
I.R.I.G.M.-B.P. 53
38041 Grenoble, FRANCE

Dr. Kin Yip Chun
Geophysics Division
Physics Department
University of Toronto
Ontario, CANADA

Prof. Hans-Peter Harjes
Institute for Geophysic
Ruhr University/Bochum
P.O. Box 102148
4630 Bochum 1, GERMANY

Prof. Eystein Husebye
NTNF/NORSAR
P.O. Box 51
N-2007 Kjeller, NORWAY

David Jepsen
Acting Head, Nuclear Monitoring Section
Bureau of Mineral Resources
Geology and Geophysics
G.P.O. Box 378, Canberra, AUSTRALIA

Ms. Eva Johannisson
Senior Research Officer
National Defense Research Inst.
P.O. Box 27322
S-102 54 Stockholm, SWEDEN

Dr. Peter Marshall
Procurement Executive
Ministry of Defense
Blacknest, Brimpton
Reading FG7-FRS, UNITED KINGDOM

Dr. Bernard Massinon, Dr. Pierre Mechler
Societe Radiomana
27 rue Claude Bernard
75005 Paris, FRANCE (2 Copies)

Dr. Svein Mykkeltveit
NTNT/NORSAR
P.O. Box 51
N-2007 Kjeller, NORWAY (3 Copies)

Prof. Keith Priestley
University of Cambridge
Bullard Labs, Dept. of Earth Sciences
Madingley Rise, Madingley Road
Cambridge CB3 OEZ, ENGLAND

Dr. Jorg Schlittenhardt
Federal Institute for Geosciences & Nat'l Res.
Postfach 510153
D-3000 Hannover 51, GERMANY

Dr. Johannes Schweitzer
Institute of Geophysics
Ruhr University/Bochum
P.O. Box 1102148
4360 Bochum 1, GERMANY